Research Paper

GEOSPHERE

GEOSPHERE; v. 13, no. 1

doi:10.1130/GES01376.1

13 figures; 3 tables; 1 supplemental file

CORRESPONDENCE: jiexu@utexas.edu

CITATION: Xu, J., Snedden, J.W., Galloway, W.E., Milliken, K.T., and Blum, M.D., 2017, Channel-belt scaling relationship and application to early Miocene source-to-sink systems in the Gulf of Mexico basin: Geosphere, v. 13, no. 1, p. 179–200, doi:10.1130/GES01376.1.

Received 7 June 2016
Revision received 26 September 2016
Accepted 14 November 2016
Published online 22 December 2016

Channel-belt scaling relationship and application to early Miocene source-to-sink systems in the Gulf of Mexico basin

Jie Xu[1,2], John W. Snedden[2], William E. Galloway[2], Kristy T. Milliken[3], and Michael D. Blum[3]

[1]Department of Geological Sciences, Jackson School of Geosciences, The University of Texas at Austin, 2275 Speedway C9000, Austin, Texas 78712, USA
[2]Institute for Geophysics, Jackson School of Geosciences, The University of Texas at Austin, 10100 Burnet Road, Austin, Texas 78758, USA
[3]Department of Geology, University of Kansas, Lawrence, Kansas 66045, USA

ABSTRACT

In past decades, numerous studies have focused on the alluvial sedimentary record of basin fill. Paleo–drainage basin characteristics, such as drainage area or axial river length, have received little attention, mostly because the paleo–drainage system underwent erosion or bypass, and its record is commonly modified and overprinted by subsequent tectonism or erosional processes. In this work, we estimate the drainage areas of early Miocene systems in the Gulf of Mexico basin by using scaling relationships between drainage area and river channel dimensions (e.g., depth) developed in source-to-sink studies. Channel-belt thickness was used to estimate channel depth and was measured from numerous geophysical well logs. Both lower channel-belt thickness and bankfull thickness were measured to estimate the paleo–water depth at low and bankfull stages.

Previous paleogeographic reconstruction using detrital zircon and petrographic provenance analysis and continental geomorphic synthesis constrains independent estimates of drainage basin extent. Comparison of results generated by the two independent approaches indicates that drainage basin areas predicted from channel-belt thickness are reasonable and suggests that bankfull thickness correlates best with drainage basin area. The channel bankfull thickness also correlates with reconstructed submarine fan dimension. This work demonstrates application to the deep-time stratigraphic archive, where records of drainage basin characteristics are commonly modified or lost.

INTRODUCTION

Drainage basin area, which controls sediment supply and water discharge to sedimentary basins, has a strong influence on sediment distribution and rock architecture in the basin (Sømme et al., 2009a; Davidson and Hartley, 2014). A quantitative analysis of paleo-drainage area for a specific unit would also provide a better understanding of sediment provenance and paleoclimate at the source terranes. However, such work on reconstructing paleo-drainage area has received less attention compared to the numerous studies focused on the alluvial sedimentary record of basin fill.

Recent advances in source-to-sink (S2S) analysis provide a method for calculating paleo–drainage basin area by examining the dimensions of sedimentary strata in the basin. The S2S analysis considers whole-sediment erosional-depositional processes as a contemporaneous and genetically linked system (Allen, 2008a; Sømme et al., 2009a, 2009b; Fig. 1). Among the components of the S2S system, tectonics and climate, acting on the drainage basin area, determine sediment supply and water discharge (Fig. 2A; Matthai, 1990; Milliman and Syvitski, 1992; Syvitski and Milliman, 2007; Allen, 2008b; Sømme et al., 2009a). Although fluvial deposits are volumetrically minor in most basin fills, the majority of the basin fill transits from source to sink through fluvial channels (Galloway, 1981; Hovius, 1998), and channel flow is thus a key link between upstream drainage basin and depositional sinks. Therefore, sediments deposited in fluvial settings should preserve critical signals that could be used to estimate the key parameters of S2S systems (Blum and Törnqvist, 2000; Blum and Womack, 2009). In this study, the term "channel belt" is used to mean both the channels defined by two adjacent river cutbanks and fluvial deposits that preserved in the three-dimensional stratigraphic record.

Studies of modern and Quaternary fluvial systems have explored the relationships among channel-belt dimensions, drainage area, and water discharge (e.g., Leopold and Maddock, 1953; Ethridge and Schumm, 1977; Matthai, 1990; Davidson and North, 2009; Blum et al., 2013). Investigation of 488 modern rivers by Syvitski and Milliman (2007), covering 63% of the global land surface, suggests a strong correlation between drainage area and river discharge (Fig. 2A). Blum et al. (2013) measured Quaternary fluvial systems in different tectono-climatic regions and found that channel bankfull depth (or channel-belt thickness) has a positive correlation with bankfull discharge (Fig. 2B). Anderson et al. (2004, 2016) documented a strong correlation between river sediment flux and drainage basin area in the late Quaternary glacioeustatic cycles in the northern Gulf of Mexico (GOM) margin.

In addition, climate has greatly affected river discharge; a humid climate could generate a relatively deep channel depth with a small water-contributing area (Feldman et al., 2005; Gibling, 2006; Davidson and North, 2009; Davidson and Hartley, 2014; Bhattacharya et al., 2016). Local studies of drainage within a specific climatic, lithologic, and hydrologic region indicate a strong correlation among drainage area, mean channel depth, and climate (Fig. 2C; Davidson and North, 2009).

To estimate the drainage basin area of an ancient system, the key is to extract correct paleo-fluvial dimensions from outcrop or subsurface data. Miall

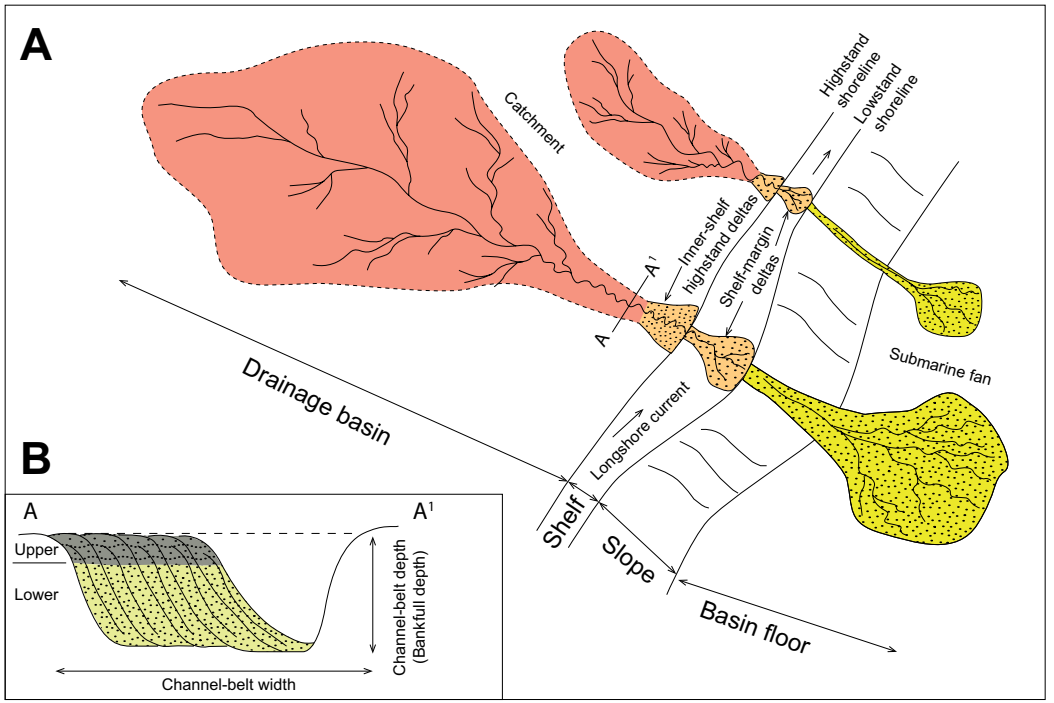

Figure 1. A simplified source-to-sink system model and channel-belt profile. (A) Large drainage systems usually produce greater sediment flux and water discharge, and thereby produce larger delta and submarine fan systems, than do smaller ones. (B) Idealized cross-section of fluvial channel deposits on a low-gradient coastal plain. Channel deposits are the stratigraphic record of the key linking pathway connecting sediment production in the source drainage basin and deposition in the deep basin.

(2006) pointed out that the vertical dimension of a channel (depth) is more easily measured from well logs, cores, or outcrops and that these measurements more reliably reflect features of ancient rivers than do river width and length estimated from limited outcrops. Some studies report that channel-belt deposits formed in bends of meandering rivers provide a good proxy estimate of paleo-channel depth (e.g., Leeder, 1973; Ethridge and Schumm, 1977; Willis, 1989). Therefore, channel depth can be estimated by measuring a completely preserved channel-bar-deposit package (Lorenz et al., 1985; Bridge and Tye, 2000; Bhattacharya and Tye, 2004; Miall, 2006; Holbrook and Wanas, 2014).

Some studies have attempted to recover drainage basin area from preserved channel deposits (e.g., Bhattacharya and Tye, 2004; Davidson and North, 2009; Davidson and Hartley, 2014). For example, Davidson and North (2009) used maximum preserved channel depth to calculate drainage area of an ancient rock unit by applying the scaling relationships derived from modern regional geomorphological curves. Knowledge of tectonic and climatic conditions in an ancient system is required for guiding the selection of suitable modern systems having similar settings. Most previous studies have proven useful in a relatively small basin within a uniform tectonic and climatic region; this scaling relationship has not been tested in large, passive-margin basins that have diverse climatic, tectonic, topographic, lithologic, and geomorphic zones.

In this work, we statistically characterize several channel-belt dimensions using well logs and then use these results to calculate paleo-drainage area by employing the scaling relationship established on modern and Quaternary fluvial systems. As a data-rich basin having well-preserved fluvial-coastal plain deposits along its northern margin, the GOM provides an opportunity to test such scaling relationships using large, reconstructed early Miocene fluvial systems. Previous drainage-basin analysis using detrital zircon U-Pb analysis (Xu et al., 2016) was used as an independent test for the reliability of the prediction. We extend our analysis to the deep basin and test the correlation between the drainage basin area, basin length, and submarine fan area and length proposed by Sømme et al. (2009a; Figs. 1 and 2D).

Our results have implications for deep-water exploration in the GOM, as lower Miocene sediment slope and basinal sandstones are one of the major deep-water reservoirs in the basin. However, fan distributions and areas are commonly masked by a structurally complex salt canopy that developed during and after Miocene deposition. Therefore, channel-belt dimensional data obtained from onshore fluvial deposits could be a useful predictor of axial length of submarine channel sands.

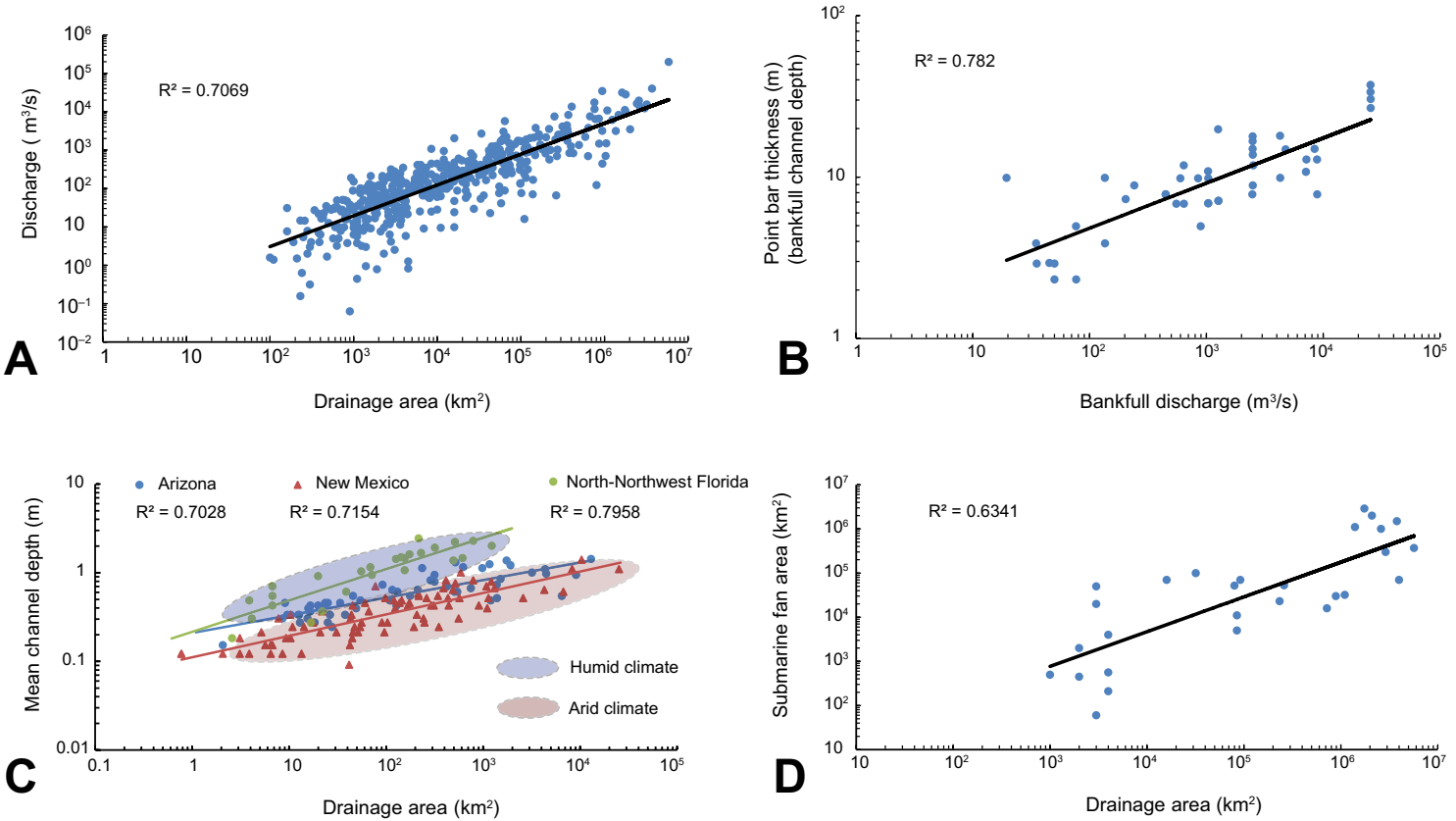

Figure 2. Scaling relationships between different components of source-to-sink systems: Correlations between river discharge and drainage area (A), bankfull discharge and channel-belt thickness (B), drainage area and mean channel bankfull depth (C), and drainage area and submarine fan area (D). Panels A to D are replotted from Syvitski and Milliman (2007); Blum et al. (2013); Moody et al. (2003) and Metcalf (2004); and Sømme et al. (2009a), respectively.

BACKGROUND

The Cenozoic GOM has been characterized by voluminous siliciclastic sediment influx from the North American hinterland to the basin. Major tectonostratigraphic phases, including Laramide, mid-Cenozoic volcanism and thermal uplift, Basin and Range, and Neogene glacial, produced four distinct sediment-routing and basin-filling histories (Fig. 3; Galloway, 2008; Galloway et al., 2011), representing the Paleocene-Eocene, Oligocene, Miocene, and Pleistocene (Fig. 3). Two of these units, the Paleocene-Eocene Wilcox Group and the Miocene, are the major hydrocarbon production units in the GOM.

The early Miocene (ca. 23–15 Ma) was a transitional period of tectonic reorganization in North America, changing from arid volcanogenic in the late Eocene to early Miocene to arid extensional in the middle to late Miocene (Fig. 3). Arid climatic conditions extended from the Western Interior to the northwest GOM margin, whereas a humid climate prevailed in the eastern GOM coastal plain and Appalachian uplands (Galloway et al., 2011). The arid climate and Rio Grande extension in the Western Interior combined to be a major cause of the decreased sediment input in early Miocene time (Fig. 3). Rejuvenation of the Appalachians in the middle Miocene, combined with the wet climate, increased the delivery of sediment to the east-central GOM through the paleo–Tennessee River. Together with the Mississippi River, the Tennessee formed a large deltaic depocenter. Consequently, the lower Miocene interval records both sediment-routing and linked depocenters shifting from the western GOM in the Paleogene to the central GOM in the Neogene (Galloway et al., 2011;

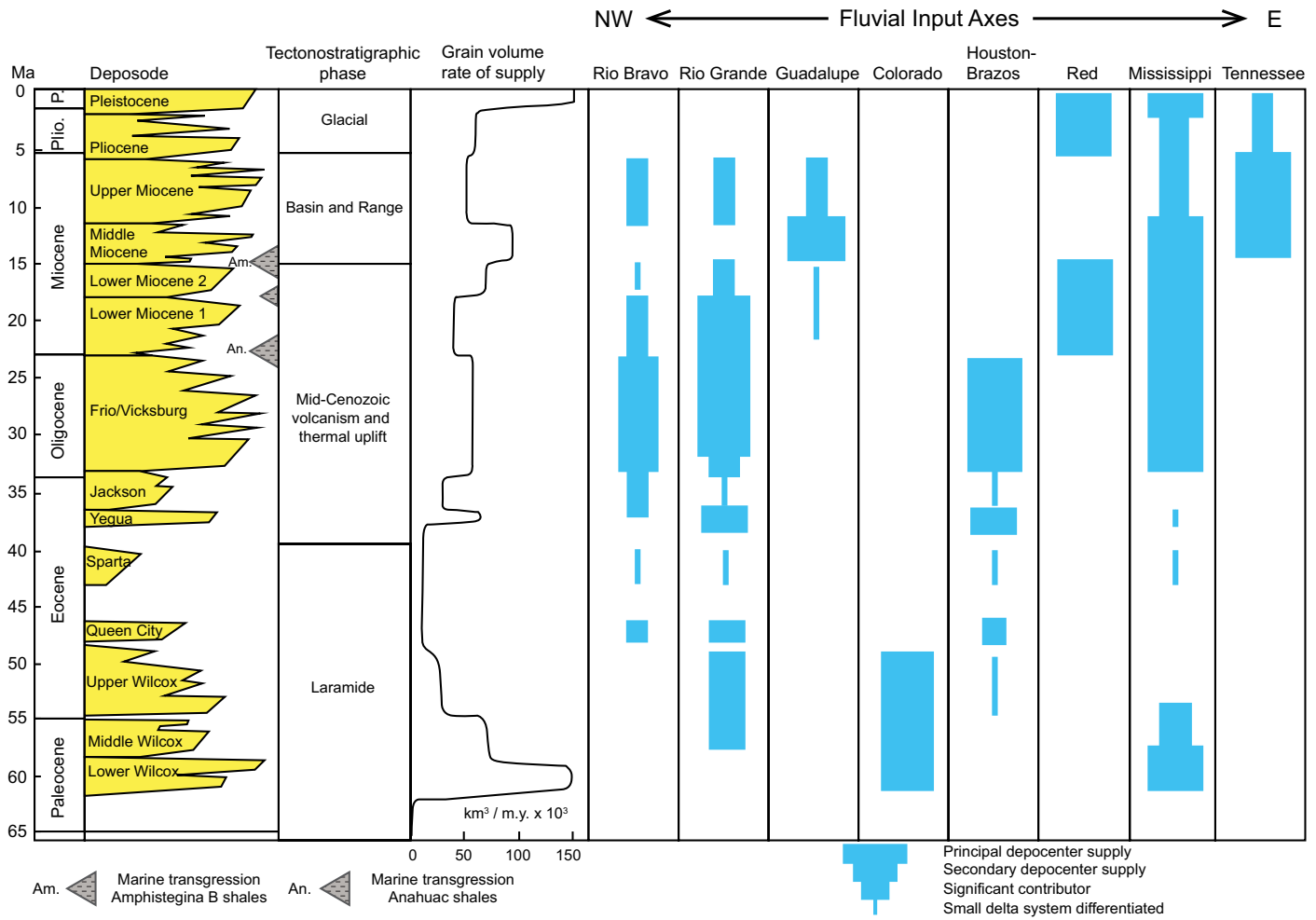

Figure 3. Depositional evolution history of the principal Cenozoic northern Gulf of Mexico fluvial axes. Columns show principal depositional episodes, major tectonostratigraphic phases, grain volume rate of sediment supply, and changing rates of supply through each fluvial input axis. The unit widths in left column are schematic presentations of the relative volumetric importance of each deposode. Modified from Galloway et al. (2011). P.—Pleistocene; Plio.—Pliocene. Lower Wilcox, Middle Wilcox, Pliocene, Pleistocene, and others are all full formal names of name units that defined by Galloway et al. (2011).

Bentley et al., 2016; Fig. 3). Recent exploration success in deep-water drilling suggests that Miocene submarine fans ran out hundreds of kilometers onto the abyssal plain.

Two major transgressive shales bound the lower Miocene depositional sequence: the Amphistegina B shales at the top and the Anahuac shales at the base (Fig. 3). Lower Miocene strata can be separated into two subunits, informally termed lower Miocene 1 (LM1) and lower Miocene 2 (LM2), by a transgressive shale dated as ca. 18 Ma (Galloway et al., 1986).

The paleogeography constructed by Galloway et al. (2011) is based upon previous studies of the Cenozoic tectono-climatic history of the North American interior (source) and the depositional record in the GOM basin (sink). This compilation indicates that in the early Miocene, the northern GOM had

multiple synchronous fluvial systems, ranging from large extra-basinal rivers to local intra-basinal streams (Galloway, 1981; Galloway et al., 2011; Figs. 3, 4, and 5). A few large rivers, including the paleo-Mississippi and paleo-Red rivers and the paleo–Rio Grande, carried voluminous sediments and deposited thick fluvial-deltaic deposits onto the coastal plain and shelf and onto linked submarine fans in the abyssal plain (Galloway et al., 2000, 2011; Galloway, 2008; Figs. 3, 4, and 5). Smaller intra-basinal streams, including the paleo-Guadalupe and paleo–Houston-Brazos rivers, were minor sediment conveyers that only built small bay-head deltas and shore zones in the northwestern GOM (Anderson et al., 2014; Figs. 3, 4, and 5).

Several differences exist between the drainage systems in the early Miocene and their modern counterparts. Detrital zircon provenance analysis

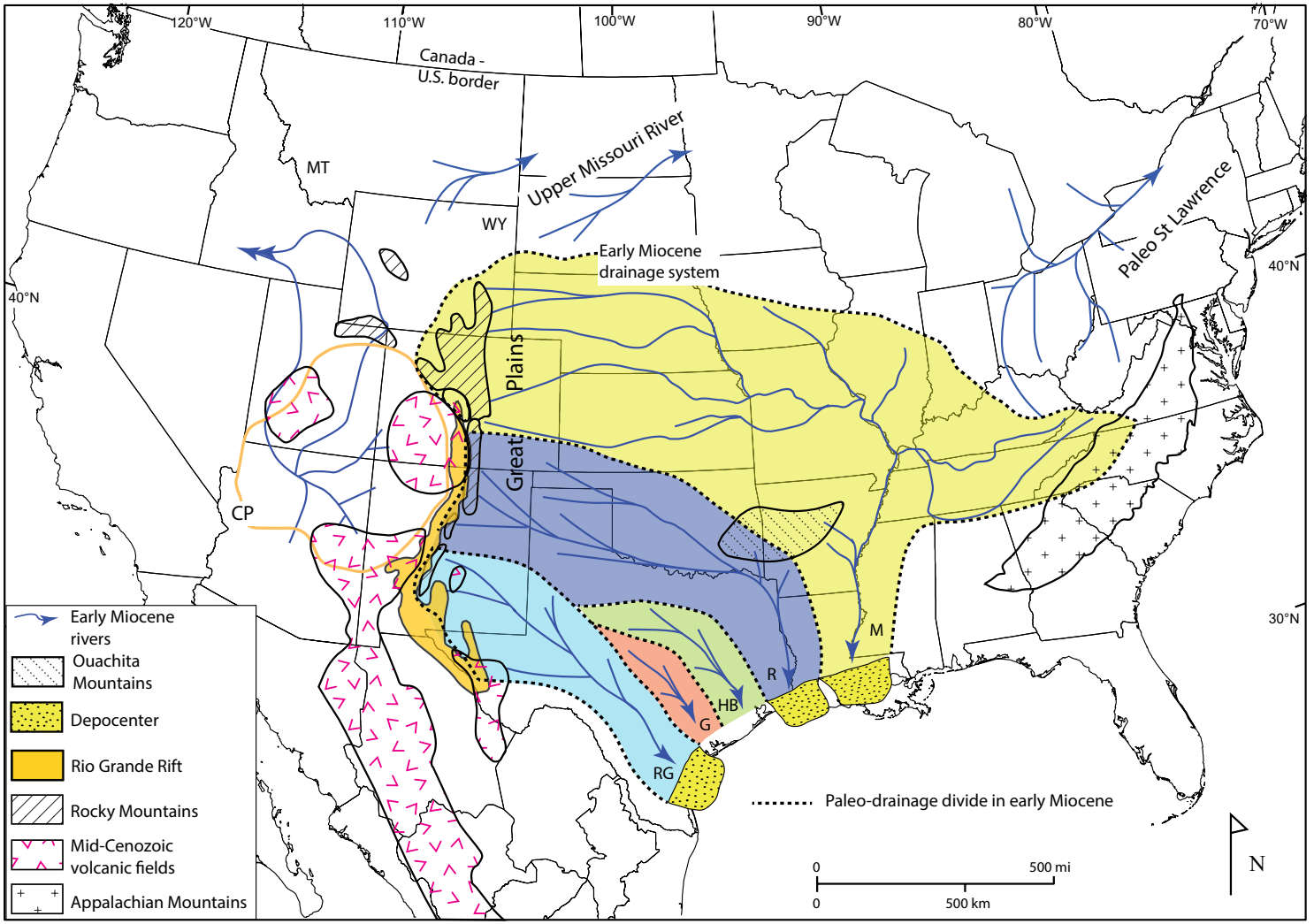

Figure 4. Paleo-drainage map of the five major fluvial axes of the early Miocene Gulf of Mexico. Modified from Galloway et al. (2011) and Xu et al. (2016). Fluvial system abbreviations: RG—Rio Grande; G—Guadalupe; HB—Houston-Brazos; R—Red; M—Mississippi. CP—Colorado Plateau; WY—Wyoming; MT—Montana.

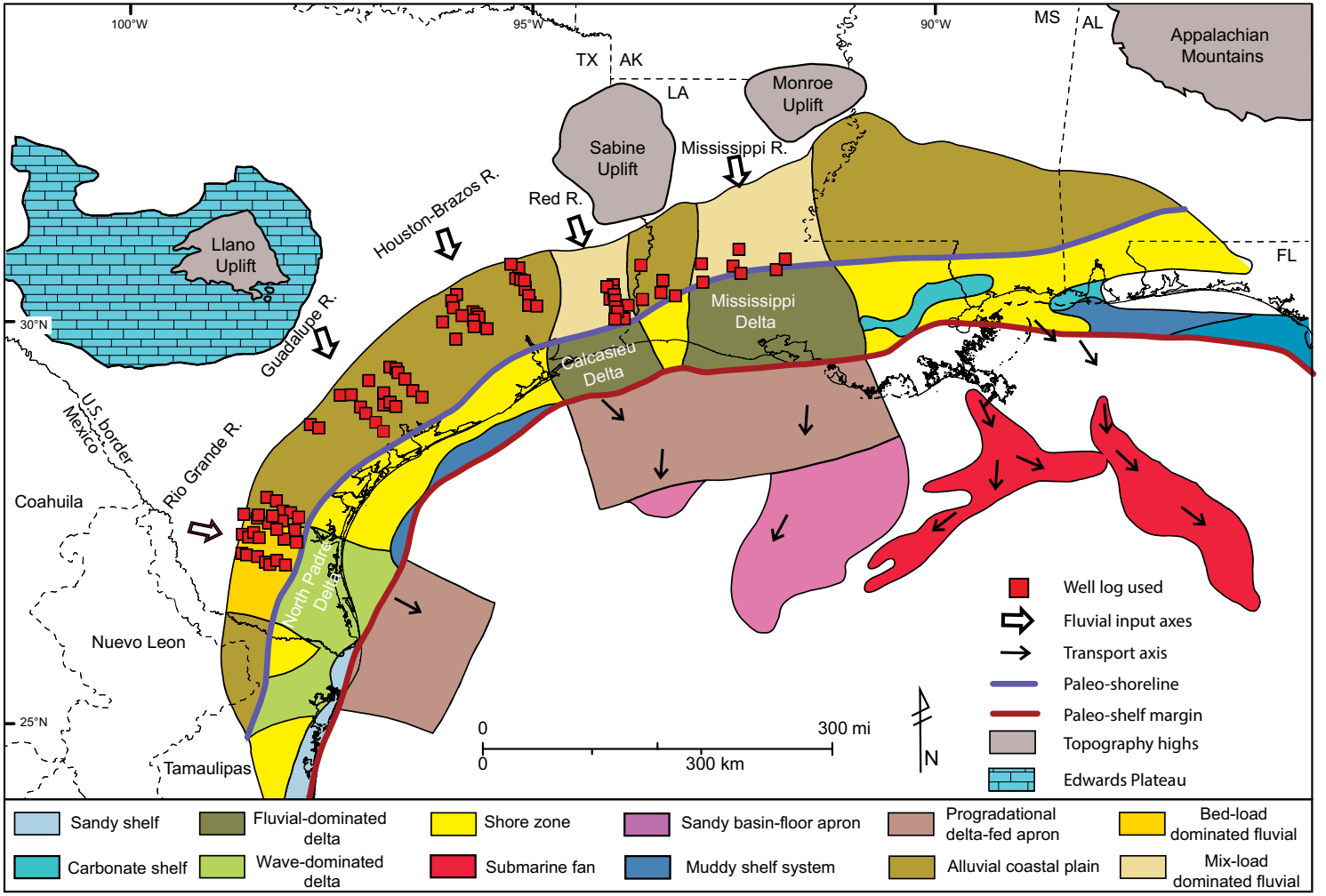

Figure 5. Well-log data set used to measure the channel-belt thickness of five major fluvial systems in the northern Gulf of Mexico. The paleogeography map of the lower Miocene interval is updated from Galloway et al. (2000) and unpublished maps of the Gulf of Mexico Basin Depositional Synthesis project atlas. R.—River; TX—Texas; AK—Arkansas; LA—Louisiana; MS—Mississippi; AL—Alabama; FL—Florida.

of lower Miocene strata suggests the presence of very limited amounts of Archean-aged zircons from corresponding basements in northern Wyoming and in Canadian shields; thus, the drainage connection between the GOM and northern Wyoming, Montana, and Canada was weak (Xu et al., 2016; Fig. 4). The paleo–Upper Missouri River and the paleo–Ohio River might have not fully integrated into a southward-flowing system until the Pliocene–Pleistocene (Galloway et al., 2011; Blum and Roberts, 2012; Bentley et al., 2016). Alternatively, the paleo–Ohio River flowed northeastward and joined the pre-glacial St. Lawrence River in the early Miocene (Hoagstrom et al., 2014, and references therein), whereas the Miocene Upper Missouri River flowed northward and merged with the pre-glaciation Bell River in Canada (Howard, 1958; Sears, 2013; Fig. 4). The Red River drained the southern Rocky Mountains (Galloway et al., 2011; Dutton et al., 2012; Xu et al., 2016) and fed the large Calcasieu delta in western Louisiana through eastern Texas (Fig. 5). Sediments deposited in

this deltaic depocenter, as much as ~2500 m thick, imply that the Red River was one of the largest fluvial systems during early Miocene time. The Red River did not merge with the Mississippi River; it was a separate fluvial system for the GOM until the Holocene (Saucier, 1994; Galloway et al., 2011).

DATABASE AND METHODOLOGY

Database

A complete succession of point-bar deposits in outcrop can be used to estimate channel depth. However, lower Miocene outcrop exposures are few and generally small, and they rarely display a complete channel-belt succession. Measurement of channel-belt thickness in this study is therefore based on subsurface well logs. Logs from 94 wells were used to measure the channel-belt thickness of five major early Miocene rivers on the GOM Coast: the paleo-Mississippi, paleo-Red, paleo–Houston-Brazos, and paleo-Guadalupe rivers, and the paleo–Rio Grande (Figs. 4 and 5).

These well logs were extracted from several publications (Spradlin, 1980; Dodge and Posey, 1981; Bebout and Gutierrez, 1983; Eversull, 1984; Galloway et al., 1986; Foote et al., 1990; Baker, 1995; Young et al., 2010, 2012). The lower Miocene boundaries are well constrained in previous publications by biostratigraphic data or by detailed well correlation based on key depositional surfaces (e.g., erosional unconformities and marine flooding surfaces) in the GOM region. Paleogeographic maps interpreted from numerous well logs, along with seismic interpretation by Gulf of Mexico Basin Depositional Synthesis (GBDS) project (University of Texas Institute for Geophysics) researchers, provide a well-defined reconstruction of the GOM coastal plain (Fig. 5). The shoreline position defined by GBDS researchers delineates the approximate boundary between fluvial and delta-marine environments (Fig. 5). Wells are located on the fluvial-coastal plain regions, landward of the paleo-shoreline. A few wells are located near the paleo-shoreline and display both marine deposits formed during a high sea-level stage and fluvial features in lowstand. Criteria for recognition of fluvial channel-belt facies and thickness measurements are discussed below.

Single-Story Channel-Belt Recognition

A river is a dynamic conduit that carries sediments from the hinterland to build coastal plains and deltas along the basin margin and in some cases even feed submarine fans on the abyssal plain. Major fluvial sediments deposited in coastal plains usually consist of channel-belt fill (lateral accretion deposits), crevasse splay, floodplain, and lake deposits (Fig. 6). Recognition of each fluvial-coastal plain depositional facies has been well established by previous works (e.g., Bernard et al., 1970; Galloway, 1981; Galloway et al., 1982; Bridge and Tye, 2000). One effective way to differentiate these facies is by using well log patterns, e.g., spontaneous (SP), gamma ray (GR), or resistivity (RT) curves. Different sedimentary facies have distinct depositional processes, producing differing lithological assemblages, grain-size trends, and mineral composition, thereby revealing different responses on geophysical well logs (e.g., Galloway, 1981; Galloway et al., 1982, 1986; Snedden, 1984; Fig. 6).

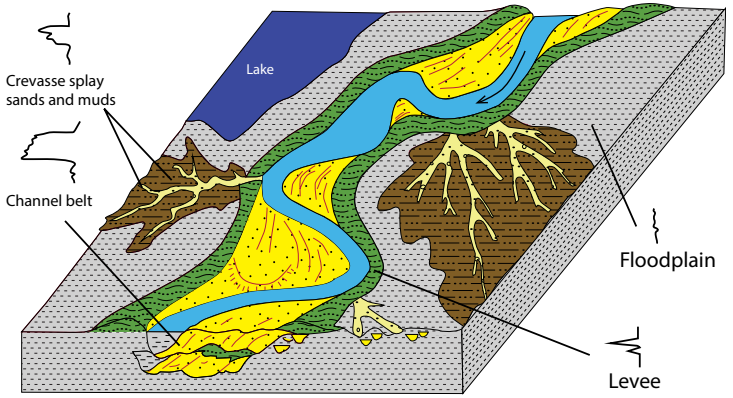

Figure 6. Schematic features of a meandering fluvial system characteristic of the early Miocene Gulf of Mexico Coast. Each sedimentary facies has distinct well-log patterns (shown). The well log patterns displayed here are gamma ray. Modified from Galloway (1981).

Channel-belt deposits, which form from migration of an active channel, are major repositories of sediments within fluvial systems. The channel filling and bar aggrading usually result from decreasing flow and decreasing water depth (Miall, 2010). Therefore, a fluvial channel-belt deposit is typically characterized by a sharply defined erosional base and an upward-fining succession, due to the decline in fluvial strength and consequent decreasing grain size upward (Fielding and Crane, 1987; Bridge and Tye, 2000; Miall, 2010; Hubbard et al., 2011; Figs. 6 and 7). Channel-belt deposits can be divided into two subunits: those of the lower channel belt, characterized by coarse-grained sandstone and large-scale trough cross-bedding at the base; and those of an upper channel belt, characterized by fine-grained sandstone, silt, andmudstone, horizontal lamination, and ripple cross-bedding at the top (Bernard et al., 1970; Bridge and Tye, 2000; Figs. 7A and 7B). It is easy to differentiate channel and bar deposits from floodplain, levee, and splay deposits, as the latter are mostly muddy and may display upward-coarsening textural trends (Galloway, 1981; Galloway and Hobday, 1996; Ambrose et al., 2009; Fig. 6). Coastal deltaic deposits usually show an upward-coarsening well-log motif and are easy to differentiate from channel-belt deposits (Olariu and Bhattacharya, 2006).

Channel belts in fluvial systems can deposit sediment by either lateral expansion or downstream translation (Bridge and Tye, 2000; Bridge, 2003; Willis and Tang, 2010; Smith et al., 2009, 2011; Ghinassi and Ielpi, 2015, 2016). The upstream channel belt deposited by lateral accretion has a high net sandstone content (Fig. 7C). The downstream channel belt is formed by downstream translation and is characterized by a heterogeneous package of sands and muds and a serrate, upward-fining log motif (Willis, 1989; Smith et al., 2009, 2011; Willis and Tang, 2010; Hubbard et al., 2011; Durkin et al., 2015; Fig. 7C).

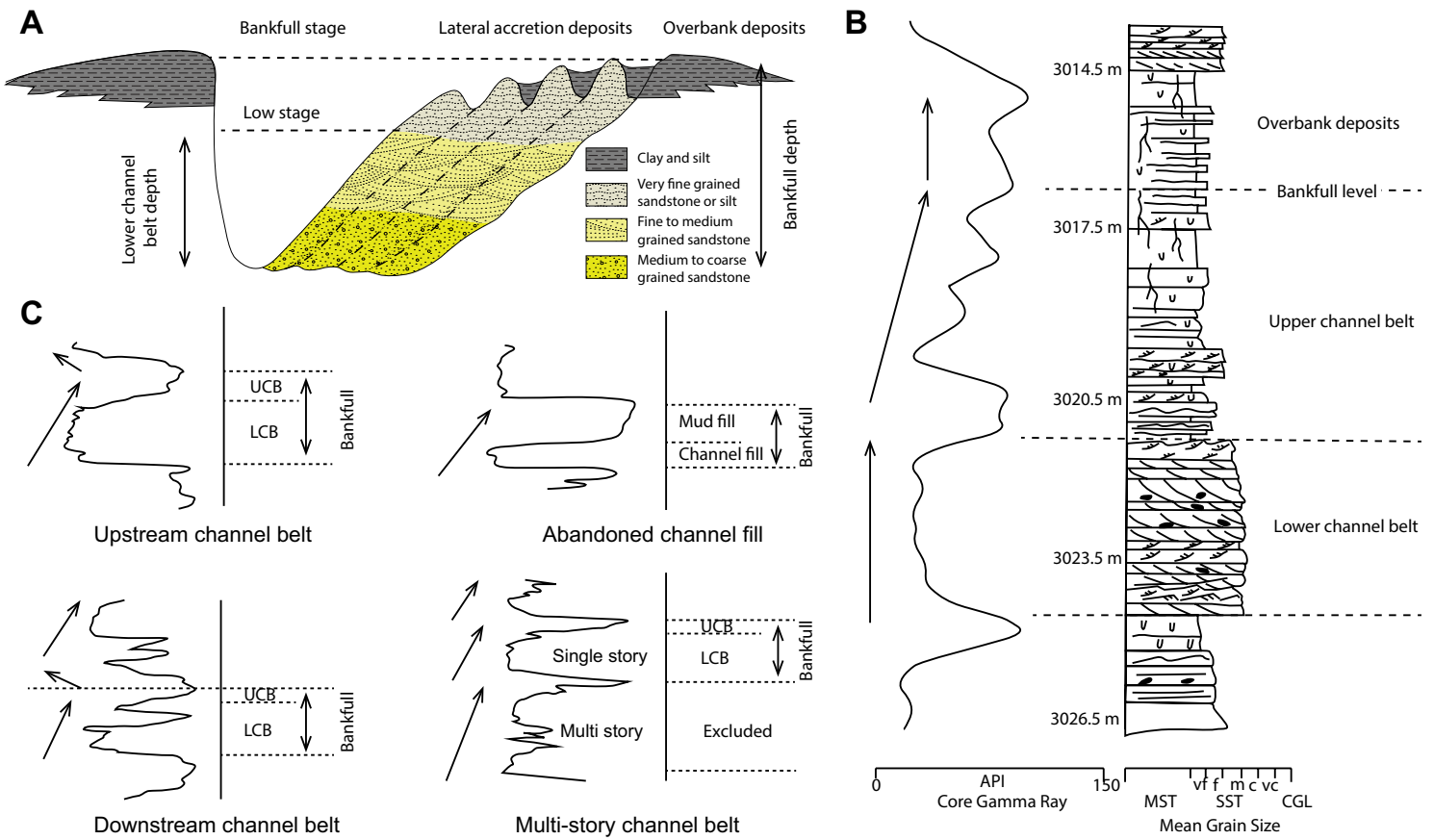

Figure 7. (A) Cross-section of channel-belt deposits. Modified from Saucier (1994). (B) Sedimentological and wireline-log features of channel-belt deposits from Travis Peak Formation, East Texas Basin. Adapted from Tye (1991) and Bridge and Tye (2000). (C) Typical well-log response patterns of lower Miocene channel-belt deposits observed in the northern Gulf of Mexico, including upstream channel belt, downstream channel belt, abandoned channel fill, and multi-story channel belt. Gamma ray well logs are used here to differentiate sandstone and mudstone. Facies recognition criteria on the well log are adapted from Bernard et al. (1970) and Bridge and Tye (2000). The arrows indicate coarsening upward or fining upward of grain size. Abbreviations: API—American Petroleum Institute; MST—mudstone; SST—sandstone; CGL—conglomerate; vf—very fine; f—fine; m—medium; c—coarse; vc—very coarse. LCB—lower channel belt; UCB—upper channel belt.

The lithological heterogeneity is likely caused by deposition of clay derived from the undercut bank by caving during flood stages, or by clay drapes deposited in channel-belt swales during flooding (Bernard et al., 1970; Davies et al., 1993). Seasonal sediment flux can also result in a heterogeneous package of sands and muds in channel-belt deposits (e.g., Labrecque et al., 2011).

When a channel is abandoned by single-meander-loop neck cutoff or by avulsion, the remaining accommodation space is usually filled by fine-grained sediments in response to resultant reduced flow energy (Bernard et al., 1970; Bridge and Tye, 2000; Blum et al., 2013). The channel fills can be either sand rich in upstream areas where the channel remains connected to the new active channel or very muddy in downstream regions located away from the active channel. Overall, the well-log SP and GR curves of channel fills are characterized by a relatively thin, blocky or bell-shaped sandstone at the base and a thick, flat shale baseline on the top (Fig. 7C).

Multi-Story Channel-Belt Deposits

The stratigraphic record is usually incomplete (Strauss and Sadler, 1989; Sadler and Jerolmack, 2015), and preservation of a complete succession of channel deposits is always a critical issue to consider when using channel-belt

thickness to estimate channel depth in the deep-time stratigraphic setting (Lorenz et al., 1985; Bridge and Tye, 2000; Miall, 2010; Holbrook and Wanas, 2014; Nicholas et al., 2016). Preservation of a channel-belt succession is highly dependent on sediment supply and accommodation space (Bridge, 2003; Gibling, 2006). The fluvial deposits tend to become amalgamated and to form multi-story sand bodies in low- accommodation settings. River avulsions usually reoccupy the previous river course by eroding and stacking upon earlier channel deposits (Blum et al., 2013). This process can sometimes make it hard to differentiate multi-story from single-story channel-belt deposits. In a rapidly subsiding basin, such as the GOM during the Cenozoic, the high accommodation rate favors a more complete preservation of channel deposits (Bridge, 2003; Gibling, 2006; Miall, 2010).

Amalgamated channel deposits usually display blocky, over-thickened, multi-story sand bodies with some embedded, thin, laminated mud layers (Fig. 7C). Thin mud layers are either the basal, mud clast–rich channel-lag deposits of an overlying channel belt or the upper, muddy part of an underlying channel belt that has not been fully eroded. The mud bed can cause SP and GR curves deflect to a shale baseline between two stacking channel-belt deposits. In our analyses, we try to avoid measuring channel-belt thickness from multi-story channel belts and instead focus upon single-story channel belts.

Channel-Belt Thickness Measurement

A complete channel-belt deposit incorporating both a sandy lower part and a muddy upper part represents a bankfull stage of river discharge that forms the channel (Wolman and Miller, 1960; Bridge and Tye, 2000; Gibling, 2006; Miall, 2014; Fig. 7A). Bridge and Tye (2000) suggested that complete preservation of a channel-fill sequence is a useful proxy for estimation of paleo-channel depth. The thickness of sandy lower channel-belt deposits (Fig. 7A) indicates the minimum constructional depth of the channel and only preserves a fraction of channel-forming discharge (Frazier and Osanik, 1961; Bridge and Tye, 2000; Miall, 2014). The lower channel-belt deposits are relatively easily recognized on SP, GR, and RT logs, because the sandy lower channel belt and the muddy upper channel belt have markedly different clay contents and thus have a different response on well-log curves (Figs. 7B and C). Bankfull thickness (a complete succession of channel-belt thickness) is relatively more difficult to measure compared to lower channel-belt deposit, because the top boundary of the muddy upper channel belt is not easily distinguished from subsequent overbank deposits by grain size and clay content. Thus, uncertainty is associated with this measurement. Upper channel-belt thickness can be either underestimated if part of the top deposit was truncated by an overlying channel, or overestimated if the near-channel overbank deposit is not differentiated.

We measure thickness of both the lower channel-belt (sand body) and bankfull deposits in this work (in a complete upward-fining succession). We define the top of bankfull deposits by observing the maximum deflection to the shale baseline on well-log curves (SP, GR, or RT; Fig. 7C). In summary, the lower channel-belt thickness is easier to measure but only preserves a fraction of channel-forming water discharge, whereas bankfull deposit thickness is interpretive but is reflective of paleo-channel depth at high flow discharge. In this work, we use both measured mean lower channel-belt and interpreted mean bankfull thicknesses to estimate the paleo-drainage area, but we do separate them in our analysis.

Drainage Basin Area Calculation

Blum et al. (2013) collected data on modern and Quaternary channel-belt thickness, river discharge, and drainage basin area from 61 rivers worldwide to establish a scaling relationship between channel depth and drainage basin area. Their work suggests that drainage basin area has a first-order control on river discharge and channel-belt dimension, and that climate plays a secondary role. In this work, we use the scaling relationship data set from Blum et al. (2013) to calculate the drainage basin area of early Miocene systems. Previous paleogeographic reconstruction using detrital zircon and petrographic provenance analysis and continental geomorphic synthesis provides independent estimates of drainage basin areas (Galloway et al., 2011; Xu et al., 2016; Fig. 4) and helps determine whether the drainage basin areas calculated from channel-belt thickness are geologically reasonable.

Fan Dimension Measurement

We also measure submarine fan dimension in the GOM to explore the relationship between sediment deposited in the basinal sink, river dimension, and drainage basin area. Data used to map Miocene submarine fan distribution in the deep-water basin were maintained in an ArcGIS database, and all measurements in this work were made using ArcGIS tools (Figs. 4 and 8). The term "apron" is used here to describe the poorly organized, line-sourced submarine slope system that fronted much of the ancient GOM shelf margin (Galloway, 1998; Figs. 4 and 8). In this work, the fan run-out length is calculated from the shelf margin to termination of the distal submarine fan or apron lobe, as appropriate to the slope system type. Submarine-fan area is measured from the maximum mapped fan or apron-facies distribution. The submarine fan systems in the eastern GOM were not measured, as they do not connect directly to any fluvial-deltaic axes; rather, they received sediment reworked along the coast or shelf edge by longshore currents before being diverted into deep water (Fig. 8; Snedden et al., 2012).

RESULTS

We measured 489 lower channel-belt and 552 bankfull thicknesses from 94 subsurface well logs that cover the major fluvial axes of the paleo-Mississippi, paleo-Red, paleo–Houston-Brazos, and paleo-Guadalupe and the paleo–Rio Grande rivers (Fig. 5; see Supplemental Materials[1]). Both the lower channel-belt and bankfull thicknesses from each river show a different frequency mode in histogram (Figs. 9 and 10). Thickness data for each river show a wide range,

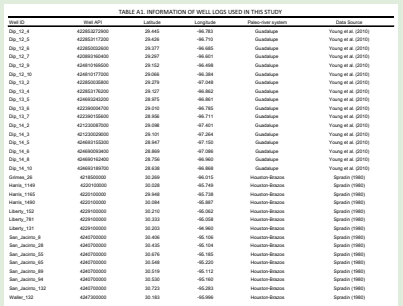

TABLE A1. INFORMATION OF WELL LOGS USED IN THIS STUDY

Well ID	Well API	Latitude	Longitude	Paleo-river system	Data Source
Dip_12_4	4208307 0560	29.445	-96.783	Guadalupe	Young et al. (2010)
Dip_12_5	4208531 17200	29.426	-96.710	Guadalupe	Young et al. (2010)
Dip_12_6	4208500 20600	29.377	-96.685	Guadalupe	Young et al. (2010)
Dip_12_7	4208931 90400	29.297	-96.601	Guadalupe	Young et al. (2010)
Dip_12_9	4240 19 66500	29.152	-96.468	Guadalupe	Young et al. (2010)
Dip_12_10	4240 19 07700	29.066	-96.384	Guadalupe	Young et al. (2010)
Dip_13_2	4226500 35800	29.279	-97.048	Guadalupe	Young et al. (2010)
Dip_13_4	4226531 76200	29.127	-96.862	Guadalupe	Young et al. (2010)
Dip_13_5	4246924 52300	28.975	-96.861	Guadalupe	Young et al. (2010)
Dip_13_6	4223900 04700	29.010	-96.765	Guadalupe	Young et al. (2010)
Dip_13_7	4223901 55600	28.956	-96.711	Guadalupe	Young et al. (2010)
Dip_14_2	4212300 87000	29.098	-97.401	Guadalupe	Young et al. (2010)
Dip_14_3	4212302 39600	29.101	-97.264	Guadalupe	Young et al. (2010)
Dip_14_5	4246931 53300	28.947	-97.150	Guadalupe	Young et al. (2010)
Dip_14_8	4246900 39400	28.869	-97.066	Guadalupe	Young et al. (2010)
Dip_14_9	4246901 62400	28.756	-96.960	Guadalupe	Young et al. (2010)
Dip_14_10	4246931 89700	28.638	-96.868	Guadalupe	Young et al. (2010)
Grimes_26	421 85200000	30.269	-96.015	Houston-Brazos	Spradlin (1980)
Harris_1149	422 01100000	30.028	-95.749	Houston-Brazos	Spradlin (1980)
Harris_1165	422 01100000	29.948	-95.738	Houston-Brazos	Spradlin (1980)
Harris_1490	422 01100000	30.084	-95.887	Houston-Brazos	Spradlin (1980)
Liberty_152	422 91100000	30.210	-95.062	Houston-Brazos	Spradlin (1980)
Liberty_781	422 91100000	30.333	-95.058	Houston-Brazos	Spradlin (1980)
Liberty_131	422 91100000	30.203	-94.960	Houston-Brazos	Spradlin (1980)
San_jacinto_8	424 70700000	30.406	-95.106	Houston-Brazos	Spradlin (1980)
San_jacinto_39	424 70700000	30.405	-95.104	Houston-Brazos	Spradlin (1980)
San_jacinto_55	424 70700000	30.676	-95.185	Houston-Brazos	Spradlin (1980)
San_jacinto_65	424 70700000	30.548	-95.220	Houston-Brazos	Spradlin (1980)
San_jacinto_89	424 70700000	30.516	-95.112	Houston-Brazos	Spradlin (1980)
San_jacinto_94	424 70700000	30.530	-95.160	Houston-Brazos	Spradlin (1980)
San_jacinto_132	424 70700000	30.723	-95.283	Houston-Brazos	Spradlin (1980)
Waller_152	424 73500000	30.183	-95.996	Houston-Brazos	Spradlin (1980)

[1]Supplemental Materials. Geophysical well log information and the lower channel-belt and bankfull thickness data measured from well logs. Please visit http://dx.doi.org/10.1130/GES01376.S1 or the full-text article on www.gsapubs.org to view the Supplemental Materials.

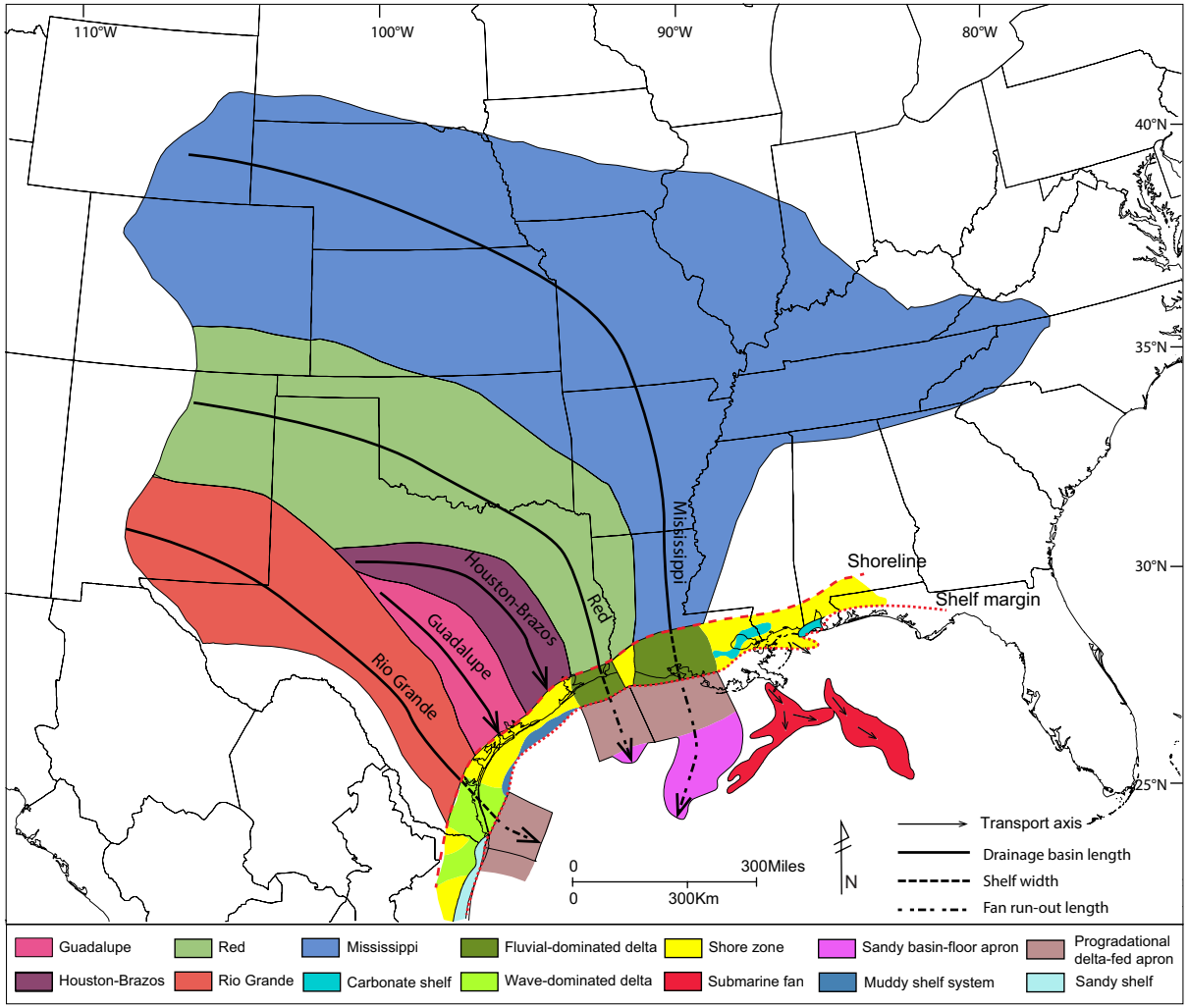

Figure 8. Paleogeographic parameters of five early Miocene sediment-routing systems, northern Gulf of Mexico, used to explore the relationships among different source-to-sink components. Fan areas were measured using the extent of slope and basin-floor apron. Modified from Galloway et al. (2000, 2011) and Xu et al. (2016).

from a few meters to >50 m (Table 1; Figs. 9 and 10). However, the thinnest 10% of the channel-belt thickness measurements are probably representing deposits of local intra-basinal rivers or side rivers near these large fluvial axes. The thickest 10% of channel-belt thickness measurements are probably representing multi-story channel deposits or valley-fill deposits. These outliers would not represent true paleo-channel depths. The remaining 80% of the channel-belt data should be more characteristic of the time-averaged fluvial channel belts recorded in deep-time archives. Therefore, we here apply a 20% filter to separate outliers, removing both the thinnest and the thickest 10% of measurements. In this study, we present both the raw data and truncated data to give a better view of channel-belt thicknesses of the five major river systems in the northern GOM (Figs. 9 and 10).

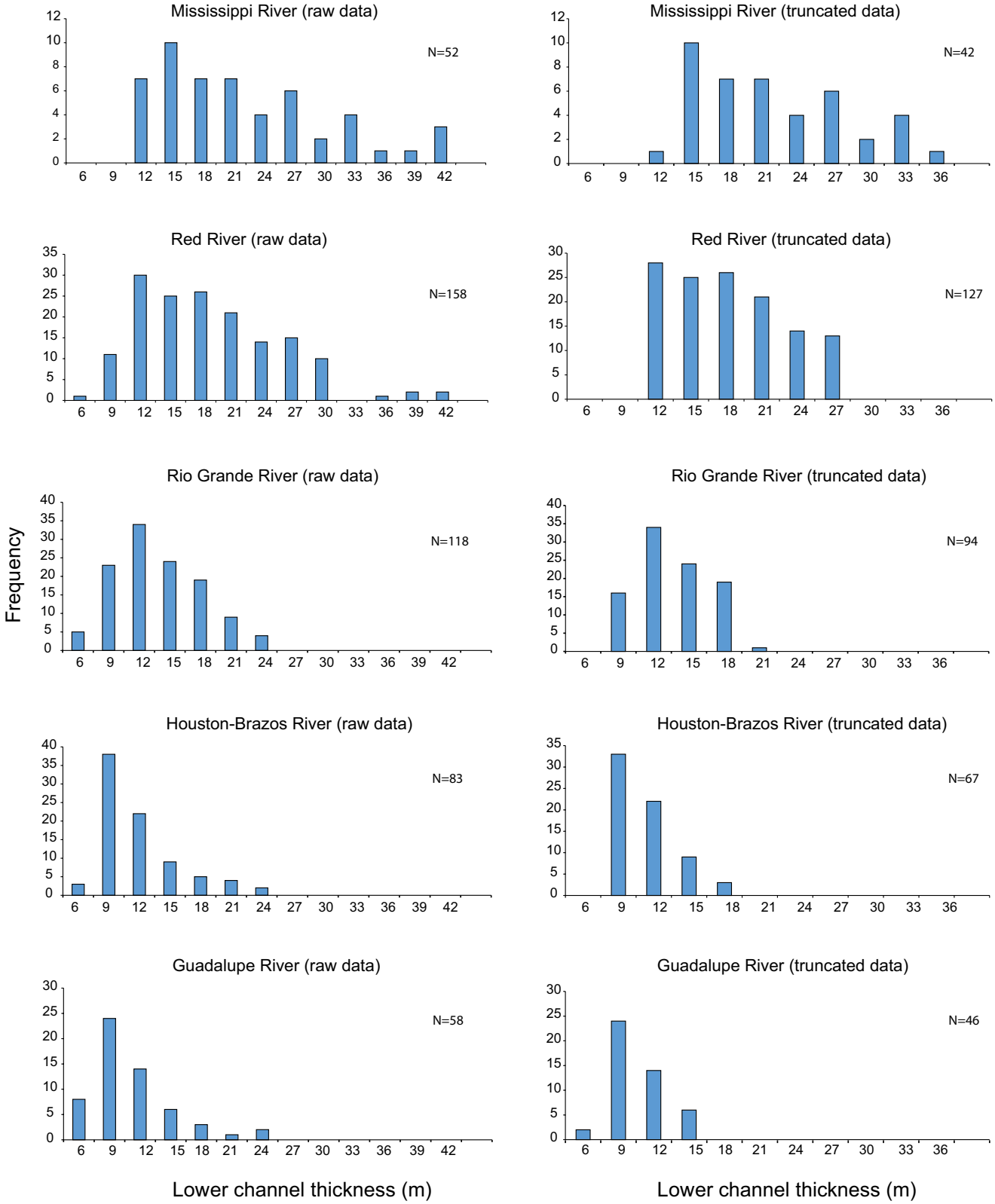

Figure 9. Histograms of lower channel-belt thickness in five Miocene fluvial systems, northern Gulf of Mexico. Truncated data exclude the thickest and thinnest 10% of measurements. N is the number of measurements.

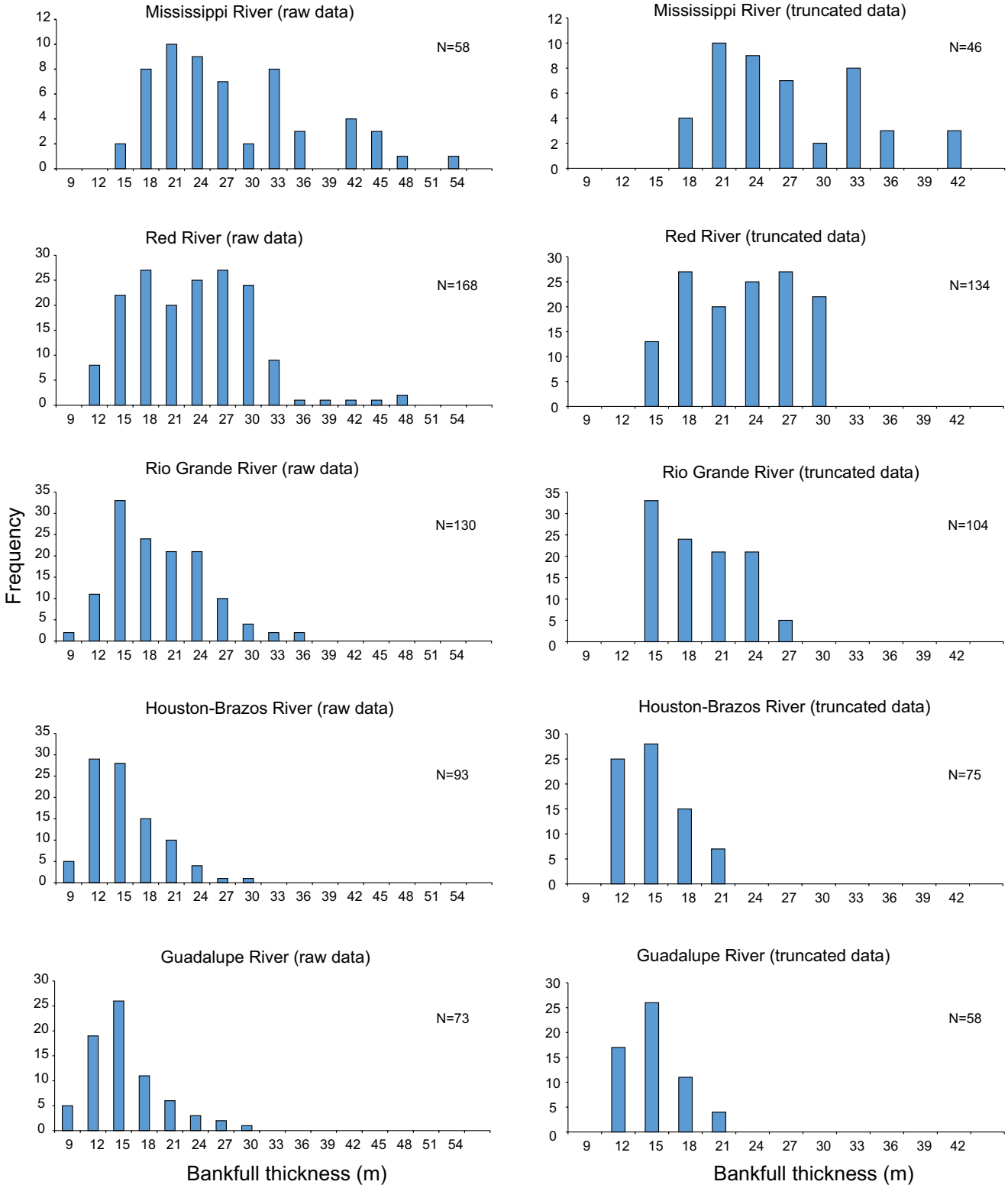

Figure 10. Histograms of bankfull thickness in five Miocene fluvial systems, northern Gulf of Mexico.Truncated data exclude the thickest and thinnest 10% of measurements. N is the number of measurements.

TABLE 1. PARAMETERS OF CHANNEL-BELT DEPOSITS MEASURED FROM FIVE MAJOR FLUVIAL SYSTEMS IN THE NORTHERN GULF OF MEXICO

River system	Lower channel-belt thickness Range (m)	Truncated lower channel-belt thickness Range (m)	Truncated lower channel-belt thickness Mean ± std. (m)	Bankfull thickness Range (m)	Truncated bankfull thickness Range (m)	Truncated bankfull thickness Mean ± std. (m)
Mississippi	9–40	10–35	19.7 ± 6.4	12–52	15–40	25.0 ± 6.6
Red	4–40	9–26	16.1 ± 4.9	9–46	13.5–29	21.1 ± 4.8
Rio Grande	4–23	6–18	11.2 ± 3.2	6–34	12–24.5	17.0 ± 3.8
Houston-Brazos	3–22	6–16	9.1 ± 2.4	6–28	9–18.5	13.0 ± 2.8
Guadalupe	3–23	5–13	8.4 ± 2.2	6–29	9–18.5	12.8 ± 2.6

std.—standard deviation.

Lower Channel-Belt Thickness

Thicknesses of lower channel belts show a wide range, 3–40 m (Fig. 9; Table 1). Each river shows a distinct channel-belt-thickness distribution. The paleo–Mississippi River data have multiple peaks, including a major peak at ~15–21 m and three secondary peaks at 24–27, 30–33, and 39–42 m (Fig. 9). The paleo–Red River data display a similar range of lower channel-belt thicknesses in comparison to the paleo–Mississippi River. However, the lower channel-belt thicknesses of the paleo–Red River are more clustered at 12–24 m, with only a few channel belts thicker than 30 m. In contrast, the paleo–Rio Grande and paleo-Brazos and paleo-Guadalupe rivers show a narrower range of channel-belt thicknesses, from 3 to 23 m (Fig. 9; Table 1). The paleo–Rio Grande shows a slightly skewed normal distribution peaking at 9–18 m, whereas the paleo-Brazos and paleo-Guadalupe rivers show a strong right-skewed pattern, with most of the lower channel-belt data peaking at ~6–15 m (Fig. 9).

Truncated thickness data exclude the highest and lowest values, causing the mean thickness not be affected by extreme values. The paleo-Mississippi has the thickest lower channel belts, ranging from 10 to 35 m, whereas most of the paleo–Red River lower channel belts are thinner, ~9–26 m. Lower channel belts of the paleo–Rio Grande and the paleo-Brazos and paleo-Guadalupe rivers are mostly thinner than 18 m (Fig. 9).

Bankfull Thickness

For the paleo–Mississippi River, the bankfull thickness plot displays a major peak at 15–27 m and two minor peaks at 30–36 m and 39–48 m (Fig. 10). Bankfull thicknesses of the paleo–Red River are clustered in thickness ranging from 9 to 33 m (Fig. 10). The bankfull thickness of the paleo–Rio Grande has a narrower range relative to the paleo–Red River and paleo–Mississippi River, with most data peaking at 12–24 m (Fig. 10). The paleo-Brazos and paleo-Guadalupe rivers have a slightly right-skewed distribution, with most data clustering at 9–15 m and a few data ranging from 21 to 30 m in the tail of the distribution (Fig. 10). Truncated data display a narrower range but distribution patterns that are still similar to those of the raw data (Fig. 10).

Comparison of Channel-Belt Thickness Patterns

Truncated lower channel-belt thickness data for each river show significant differences in statistics and on cumulative frequency plots (Fig. 11A; Table 1). The paleo–Mississippi River yielded a relatively gentle slope in its cumulative percentage plot; lower channel-belt thickness ranges from 10 to 35 m. Truncated data have an average lower channel-belt thickness of 19.7 m, with a

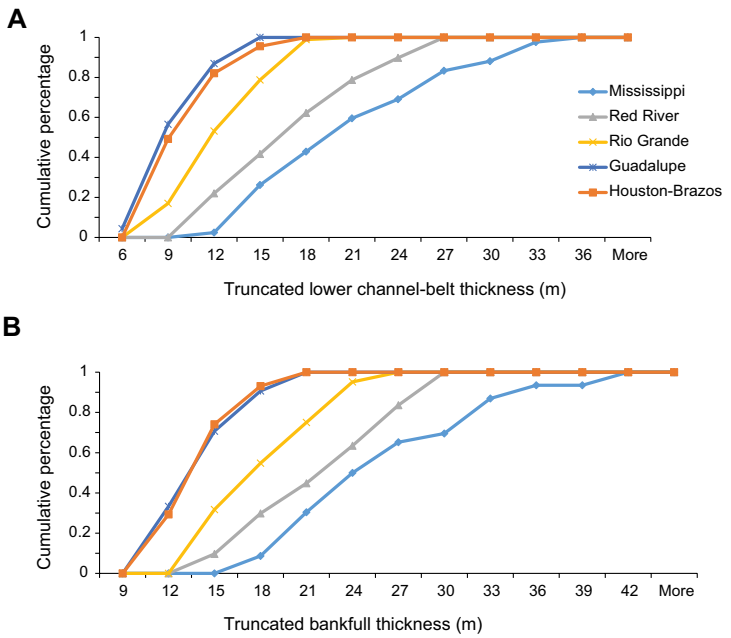

Figure 11. Comparative cumulative frequency plots of lower channel-belt thickness (A) and truncated bankfull thickness (B) in five fluvial systems in the northern Gulf of Mexico. The plots reveal distinct thickness distribution patterns in the five fluvial systems.

standard deviation of 6.4 m (Table 1). The paleo–Red River displays a similar pattern, but the data from thinner lower channel belts range from 9 to 26 m. The paleo–Red River has an average lower channel-belt thickness of 16.1 ± 4.9 m (Table 1). In contrast to the paleo-Mississippi and paleo-Red rivers, the paleo-Brazos and paleo-Guadalupe rivers are dominated by lower channel-belt thicknesses ranging from 6 to 18 m (Fig. 11A). They have an average lower channel-belt thickness of 9.1 ± 2.4 m and 8.4 ± 2.2 m, respectively (Table 1). The paleo–Rio Grande is intermediate between the large paleo-Mississippi and paleo-Red rivers and the intra-basinal paleo-Guadalupe and paleo-Brazos rivers, with lower channel-belt thicknesses ranging from 6 to 18 m and an average lower channel-belt thickness of 11.2 ± 3.2 m (Fig. 11A; Table 1).

The truncated bankfull thickness of each river displays a pattern similar to that of lower channel-belt thickness in statistics and in the cumulative frequency plot (Fig. 11B; Table 1). The paleo–Mississippi River has an average thickness of 25.0 ± 6.6 m, characterized by a gentle slope on a cumulative frequency plot (Fig. 11B). Compared to the paleo–Mississippi River, the paleo–Red River and paleo–Rio Grande have thinner bankfull thicknesses, averaging 21.1 ± 4.8 m and 17.0 ± 3.8 m, respectively (Table 1). The paleo–Houston-Brazos and paleo-Guadalupe rivers have steep slopes on their cumulative frequency plots, their average thicknesses being 13.0 ± 2.8 m and 12.8 ± 2.6 m, respectively (Fig. 11B; Table 1). Similar patterns are reproduced on the histogram plots of bankfull thickness of each river (Figs. 9 and 10).

The distinct mean and range of channel-belt thickness of each river (Figs. 9, 10, and 11; Table 1), together with previous work on fluvial input axes (Fig. 3), suggest three scales of river dimension. We categorize these river systems into three classes: continental-scale river with mean bankfull thickness of >25 m or mean lower channel-belt thickness of >20 m (e.g., the paleo–Mississippi River), large-scale river with mean bankfull thickness of 15–25 m or mean lower channel-belt thickness of 10–20 m (e.g., the paleo–Red River and paleo–Rio Grande), and moderate-scale river with mean bankfull thickness <15 m or mean lower channel-belt thickness <10 m (e.g., paleo–Brazos and paleo-Guadalupe rivers). Features of each class are discussed in the next section.

DISCUSSION

Channel-Belt Thickness Related to Drainage Basin Area

Fluvial geomorphological data collected from modern and Quaternary systems suggest a strong correlation between drainage area and channel depth (Blum et al., 2013). In our work, we also used modern and Quaternary data to constrain predicted drainage area (Fig. 12). Both mean lower channel-belt thickness and mean bankfull thickness data were used to calculate drainage basin area (Fig. 12; Table 2). The drainage area predicted from the mean lower channel-belt thickness is much smaller than the prediction from the mean bankfull thickness. The maximum predicted drainage area is ~30 times larger than the minimum prediction, e.g., for the paleo–Mississippi River (1880 × 10^3 km^2 versus 66 × 10^3 km^2 using lower channel-belt thickness; Table 2).

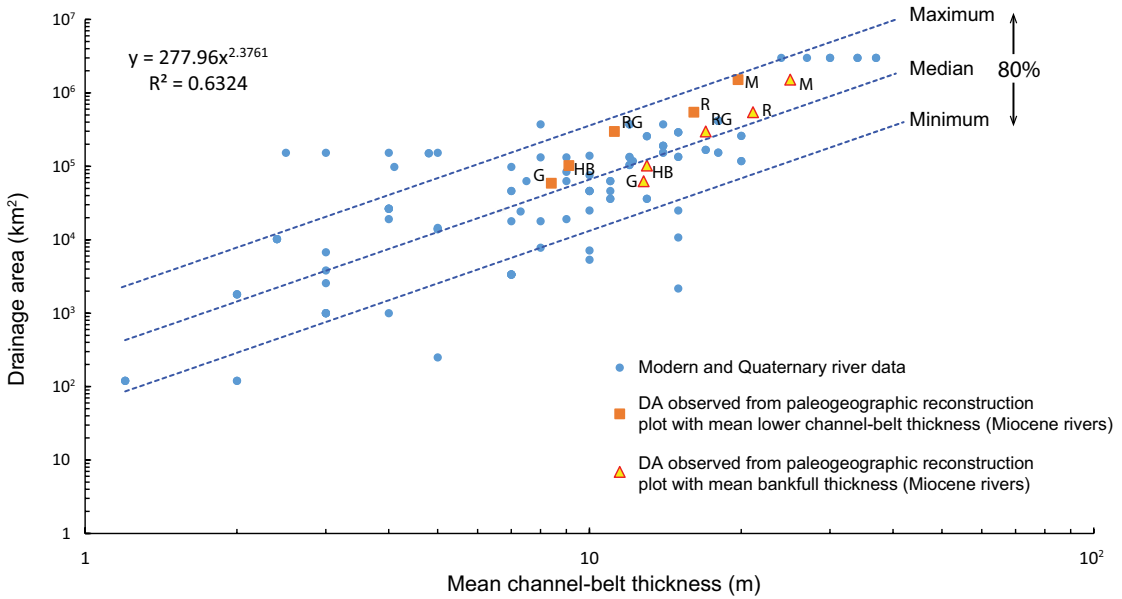

Figure 12. Correlation of drainage basin area (DA) with mean channel-belt thickness for five early Miocene fluvial systems, northern Gulf of Mexico, compared to the global scaling relationship established for modern and Quaternary systems. Previous paleogeographic work by Galloway et al. (2011) and Xu et al. (2016) provides an additional constraint on drainage basin area to test predictions. The modern and Quaternary systems data are from Blum et al. (2013). The median regression line is generated by the whole data set of modern and Quaternary systems. The maximum and minimum lines incorporate 80% of data that concentrate toward the median line. The early Miocene data set fit well with the trend of modern and Quaternary river systems. Fluvial system abbreviations: RG—Rio Grande; G—Guadalupe; HB—Houston-Brazos; R—Red; M—Mississippi.

TABLE 2. DRAINAGE BASIN AREA ESTIMATED FROM LOWER CHANNEL BELT AND CHANNEL BANKFULL THICKNESS AND FROM PALEOGEOGRAPHIC RECONSTRUCTION, NORTHERN GULF OF MEXICO

River system	Mean thickness (m)	Minimum predicted DA (10^3 km^2)	Maximum predicted DA (10^3 km^2)	Median predicted DA (10^3 km^2)	Paleogeographic reconstruction DA (10^3 km^2)	Difference (%)
Lower channel belt						
Mississippi	19.7	66	1880	330	1500	354
Red	16.1	41	1160	200	540	170
Rio Grande	11.2	17	490	86	300	249
Houston-Brazos	9.1	10	300	53	100	89
Guadalupe	8.4	9	250	44	62	41
Channel belt bankfull						
Mississippi	25.0	120	3310	580	1500	159
Red	21.1	80	2210	390	540	39
Rio Grande	17.0	50	1320	230	300	30
Houston-Brazos	13.0	25	700	123	100	19
Guadalupe	12.8	24	670	119	62	48

DA—drainage area.
Note: Difference is calculated based on DA predicted from mean channel depth and observed from paleogeographic reconstruction.

The mapped drainage basin areas from paleogeographic reconstructions of Galloway et al. (2011) and Xu et al. (2016) lie within the range of the drainage basin areas predicted from both mean lower channel-belt and mean bankfull thicknesses (Fig. 12; Table 2), indicating that such prediction based on channel depth is geologically reasonable. In addition, the correlation between channel dimension and reconstructed drainage area agrees with the trend of modern and Quaternary rivers (Fig. 12). However, the reconstructed drainage basin areas show large deviations from the median trend of modern and Quaternary systems when plotted with mean lower channel-belt thickness, whereas it shows a better correlation with mean bankfull thickness (Fig. 12). In addition, the difference between reconstructed drainage area and median predicted value from mean lower channel-belt thickness (41%–354%) is much larger than that from mean bankfull thickness (19%–159%; Table 2).

These results indicate that mean bankfull thickness better reflects drainage basin area. The sandy lower channel belt, although easily identified from subsurface well logs and outcrops, only preserves a fraction of bankfull channel depth that scales with water discharge through the channel. In addition, the lower channel-belt thickness varies from upstream to downstream (Fig. 7C), while bankfull thickness are relatively consistent in different parts of river system. Wolman and Leopold (1957) and Wolman and Miller (1960) defined bankfull flow as the most effective flow stage in maintaining channel dimensions and profiles over time. Therefore, bankfull thickness that incorporates both sandy lower and muddy upper channel belt, although in some cases more difficult to define on well logs, appears to be more sensitive to water discharge and thus drainage basin area. Therefore, in this work we focus on using mean bankfull thickness to predict drainage basin area.

Continental-Scale River (Paleo–Mississippi River)

The paleo–Mississippi River was the most important sediment routing system in the early Miocene GOM (Fig. 3; Galloway et al., 2000, 2011). The paleo–Mississippi River bankfull thickness ranges from 15 to 40 m and has an average thickness of 25 m (using the truncated data; Fig. 10; Table 1). The maximum bankfull thickness, 40 m, is close to the modern Mississippi channel depth. The bankfull depth of the modern Mississippi River ranges from 30 to 40 m (Frazier and Osanik, 1961; Saucier, 1994). Cox et al. (2014) interpreted the paleo-depth of the lower Mississippi River valley of Pliocene age as 35 m. Early Miocene Mississippi bankfull thickness is thus ~60%–70% that of the Pliocene and modern Mississippi rivers.

The maximum drainage basin area calculated from mean bankfull thickness using global modern and Quaternary river data is ~3000 × 10^3 km^2, which is close to the area of the modern Mississippi River, whereas the minimum prediction, ~120 × 10^3 km^2, approximates the that of the modern Brazos River (Fig. 12; Table 2). The maximum prediction is ~30 times larger than the minimum prediction. The median predicted drainage area lies between minimum and maximum, 580 × 10^3 km^2 (Fig. 12; Table 2).

The continental reconstruction combined with detrital zircon U-Pb ages suggests that the early Miocene Mississippi sediments were primarily sourced from the Rocky Mountains and Great Plains in the west, the Ouachita Mountains in the north, and the Appalachian Mountains and foreland basin in the east (Galloway et al., 2011; Xu et al., 2016; Figs. 4 and 8). The paleo-drainage was similar to that of the modern Mississippi River. However, the Upper Missouri River and Ohio River were not integrated into the Mississippi River until the Pliocene (Blum and Roberts, 2012; Bentley et al., 2016). Absence of

an Upper Missouri River draining northern Wyoming and southern Canada is supported by the rarity of Archean zircons in lower Miocene strata deposited in the coastal plain (Xu et al., 2016). Therefore, the reconstructed drainage area of the paleo-Mississippi is ~1500 × 10^3 km^2 (Table 2).

The reconstructed drainage area of the paleo-Mississippi lies between the median and maximum predicted drainage area from mean bankfull thickness, validating that such a prediction is reasonable; however, the uncertainty is more than an order of magnitude. The mean bankfull thickness of the early Miocene Mississippi River is ~60%–80% of that of the modern Mississippi (25 m versus 30–40 m), and consequently the drainage area of the early Miocene Mississippi River is ~50% of its modern counterpart (1500 × 10^3 km^2 versus 3300 × 10^3 km^2). The consistent relationship between channel depth and drainage area in the early Miocene and the modern system also supports the use of the modern data set to predict the ancient, unmappable drainage basin area. The general agreement between two independent approaches increases the confidence level of current understanding of the paleo-Mississippi drainage basin.

Large-Scale River (Paleo–Red River and Paleo–Rio Grande)

The paleo–Red River was a major sediment carrier in the early Miocene. It built the Calcasieu delta near the Texas-Louisiana state boundary (Galloway et al., 2000, 2011; Fig. 5). The bankfull thickness of the paleo–Red River ranges from 13.5 to 29 m, with an average thickness of 21.1 m (Fig. 10; Table 1). The paleo–Red River has the second thickest channel-belt deposit in the northern GOM coastal plain (Figs. 9, 10, and 11). The bankfull thickness of the paleo–Red River, now a tributary of the modern Mississippi River system, is much thicker than that of the modern Red River (8–18 m). The drainage area calculated from mean bankfull thickness ranges from 80 × 10^3 km^2 to 2210 × 10^3 km^2, with median value of 390 × 10^3 km^2 (Table 2).

Detrital zircon provenance analyses show that most paleo–Red River sediment was derived from the southern Rocky Mountains, southern Great Plains, eastern margins of volcanic fields in southwestern North America, and the Ouachita Mountains (Xu et al., 2016; Fig. 4). The reconstructed paleo-Red provenance suggests a drainage basin area of 540 × 10^3 km^2 (Fig. 12; Table 2).

The geologically mapped paleo-Red drainage area lies between the median and maximum predicted drainage area, and the difference between median predicted drainage area and reconstructed drainage area is 39% (Fig. 12; Table 2). The general agreement between two independent approaches indicates that the scaling relationship built for modern and Quaternary data applies well to this ancient system.

The paleo–Rio Grande was a bedload-dominated extra-basinal river that drained lithologically diverse source terranes with abundant volcanic rocks (Galloway, 1981; Galloway et al., 1982, 2011). It prograded across the shelf, built a large North Padre delta, and fed sediments into a deep-water basin (Fig. 4), indicating a large sediment influx and drainage basin area. The paleo–Rio Grande has a medium channel-belt dimension among river systems on the northern GOM coastal plain (Figs. 9, 10, and 11). Bankfull thickness ranges from 12 to 24.5 m and has an average thickness of 17 m. The calculated drainage basin area is from 50 × 10^3 km^2 to 1320 × 10^3 km^2, with a median value of 230 × 10^3 km^2 (Fig. 12; Table 2).

Detrital zircon analyses of lower Miocene strata on the South Texas coastal plain suggest that most zircons were sourced from volcanic fields from southwestern North America (Xu et al., 2016). This conclusion is also supported by petrographic analyses that show that volcanic fragments are the dominant rock fragments (Dutton et al., 2012). Reconstructed paleogeographic maps show a possible a drainage basin area of 300 × 10^3 km^2 (Fig. 4). The mapped drainage area is within the range of maximum and minimum predicted drainage basin areas (Fig. 12; Table 2). The drainage area difference between the two independent methods is 30% (Table 2), indicating that the predicted drainage area is reasonable.

Moderate-Scale Rivers (Paleo–Houston-Brazos and Paleo-Guadalupe Rivers)

The paleo–Houston-Brazos and paleo-Guadalupe rivers were two moderate-scale river systems in the early Miocene paleo-drainage network. No large deltas were built outboard of the coastal plain (Fig. 4). Mean bankfull thicknesses of the paleo–Houston-Brazos and paleo-Guadalupe rivers are ~13 m. On cumulative frequency plots, they clustered on the left side and have a steep slope with thickness data ranging from 21 to 9 m (Fig. 11B).

The drainage area for each of the two paleo-rivers calculated from mean bankfull thickness of 13 m is from ~25 × 10^3 km^2 to ~700 × 10^3 km^2, with a median value of ~120 × 10^3 km^2 (Fig. 12; Table 2). Galloway (1981) defined the paleo–Brazos-Houston and paleo-Guadalupe rivers as basin-fringe to intra-basinal streams. Sandstones in the eastern Texas coastal plain contain abundant carbonate rock fragments provided by a proximal sediment source from the elevated Edwards Plateau (west-central Texas; Galloway et al., 1982; Galloway et al., 2011; Dutton et al., 2012). The paleo-Brazos drainage basin is ~100 × 10^3 km^2, according to provenance analysis (Figs. 4 and 8; Table 2). The paleo-Guadalupe system has mixed sediments, sourced from carbonate material from the Edwards Plateau and reworked volcanic materials, and it has a drainage basin area of 62 × 10^3 km^2 (Figs. 4 and 8; Table 2).

Reconstructed drainage areas of the paleo–Houston-Brazos (100 × 10^3 km^2) and paleo-Guadalupe (62 × 10^3 km^2) lie within the range of the calculated drainage areas (~25–700 × 10^3 km^2; Table 2; Fig. 12), and the difference between calculated median drainage area and reconstructed area is 19%–48% (Table 2; Fig. 12). These agreements suggest that the scaling correlation between channel depth and drainage area from global river data is applicable to moderate-scale ancient river systems. In addition, the modern Brazos River has recorded a deeper channel depth (17–20 m; Bernard et al., 1970) and larger associated drainage area (116 × 10^3 km^2) than the early Miocene Brazos River, displaying a consistent correlation from Miocene to modern systems.

Scaling Relationships among Source-to-Sink Components

All components in source-to-sink (S2S) systems are thought to be genetically linked, and the dimension of one component should scale to other components if the whole system is in equilibrium (Sømme et al., 2009a; Romans and Graham, 2013; Bentley et al., 2016; Bhattacharya et al., 2016; Romans et al., 2016; Fig. 1). Sediment volume transferred by rivers is significantly influenced by the area, relief, lithology, and climate of the catchments, and in turn it affects the dimensions of depositional components in the basinal sink, such as submarine fan dimensions (Hovius and Leeder, 1998; Syvitski and Milliman, 2007; Covault et al., 2012; Holbrook and Wanas, 2014; Bhattacharya et al., 2016). In this work, we measured additional components of S2S systems, including submarine fan run-out length and area, and drainage basin length, to explore the relationships among these different components in S2S systems (Fig. 8).

A correlation exists between mean bankfull thickness and drainage basin area of the five early Miocene fluvial systems studied here (Fig. 13B). Sømme et al. (2009a) suggested that the length of the longest river channel increases with expanding drainage basin area. However, in an ancient system, it is difficult to measure the river length directly. Alternatively, it is more practical to measure the drainage basin length as a proxy for the longest river length

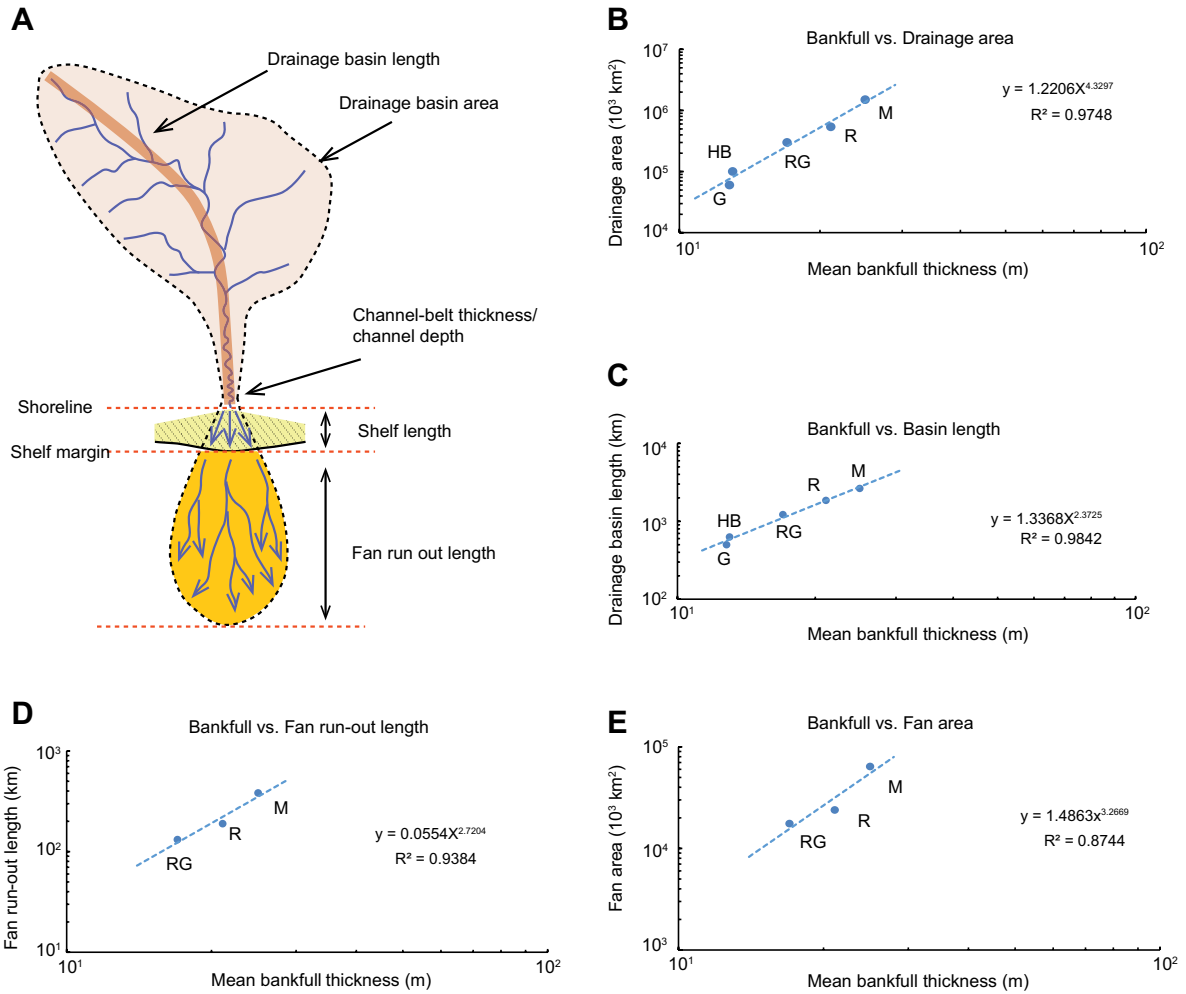

Figure 13. Relationship between mean bankfull thickness and different source-to-sink (S2S) components of five early Miocene fluvial systems, northern Gulf of Mexico. (A) A simplified S2S model illuminates the scaling parameters for different components of the system. (B) and (C) Correlations among mean bankfull thickness, drainage basin length, and drainage basin area. (D) and (E) Correlations among mean bankfull thickness, submarine fan run-out length, and submarine fan area. The correlations are based on few data, and more data collected from ancient systems will refine this relationship. Fluvial system abbreviations: RG—Rio Grande; G—Guadalupe; HB—Houston-Brazos; R—Red; M—Mississippi.

(Figs. 8 and 13A). Drainage basin length should scale to the water discharge of the entire basin and thus relate to the bankfull thickness. The drainage basin length of the five early Miocene systems displays a linear correlation with mean bankfull thickness (Fig. 13C). More data collected from ancient systems in the GOM would further test and refine this relationship.

Submarine fan run-out length and area were calculated for three mapped lower Miocene fan or apron systems, corresponding to the paleo–Mississippi River, paleo–Red River, and paleo–Rio Grande (Fig. 8). These three systems are characterized by progradation of the shelf margin and deposition in the deep-water basin by turbidity flows. Although the distribution of these basin-floor fans was mapped by GBDS project researchers by using well-log and seismic data, uncertainties remain about the exact fan run-out length and fan area in the deep-water basin. Due to the presence of a complicated salt canopy in the GOM, even after decades of explorations of lower Miocene deep-water reservoirs, the dimensions of lower Miocene submarine fans beneath salt canopy are still being mapped. No submarine fans are observed in front of the paleo–Houston-Brazos and paleo-Guadalupe fluvial systems. This may be a product of their relatively low sediment supply rate, of storage of most sediment as shoreface, shelf, and growth-faulted upper slope deposits (Fig. 5), or of masking of fan deposits beneath the complicated salt canopy.

Dimensions of the fan systems show correlation with mean bankfull thickness (Table 3; Figs. 13D and 13E). The paleo-Mississippi fan system extends across the abyssal plain 380 km from the coeval shelf margin and covers an area of 64,000 km^2. The early Miocene Mississippi fan length is shorter than that of the modern system, which has a fan run-out length of 655 km. The fan length difference is consistent with the observed channel-belt thickness of the early Miocene Mississippi fluvial system, which was ~60%–80% of the thickness of the modern system (25 m versus 30–40 m), and an early Miocene drainage area that was ~50% of that of the modern system (1,500 × 10^3 km^2 versus 3,000 × 10^3 km^2). In addition, the area of the early Miocene Mississippi fan is ~64,000 km^2 (Table 3), much smaller than that of the modern system, which has an area of 300,000 km^2 (Sømme et al., 2009a). The fan run-out distance of the paleo–Red River system (190 km) is about half of that of the paleo-Mississippi system, whereas the paleo–Rio Grande has a submarine fan run-out length of only 130 km, which is about one-third of the paleo-Mississippi fan run-out length (Table 3). The paleo–Red River and paleo–Rio Grande systems have smaller fluvial and fan dimensions compared to the paleo-Mississippi, due to their smaller drainage areas. Therefore, the dimensions of the early Miocene and modern submarine fans in the GOM scale with their onshore river dimension and drainage area, which is consistent with the mass-balance assumption in S2S, provided there is no significant intermediate storage or loss of sediment mass.

Uncertainties and Limitations

Most quantitative or semiquantitative S2S studies were based on modern or Quaternary data (e.g., Wetzel, 1993; Sømme et al., 2009a, 2009b), with few current applications to deep-time stratigraphy. When applying a scaling relationship derived from modern systems to rock records, several uncertainties and limitations are associated with the method.

Uncertainties can arise from morphological variations in a single channel. A single channel belt can have large variations in thickness by at least a factor of two during channel- forming processes (Bridge and Tye, 2000). For example, the thalweg depth can be significantly larger than the thickness of the channel belt that was deposited on the depositional bank (e.g., Fisk, 1944; Willis and Tang, 2010).

The measurement of a complete succession of channel-belt deposits to estimate paleo-channel depth is difficult to do by using well logs alone, because the upper channel deposit may be either partially truncated by an overlying channel or mixed with overbank deposits (e.g., Lorenz et al., 1985). Combing of outcrop and core data would increase the precision of measurement. The lower channel belt is sand and gravel rich and easier to identify from outcrop, core, and well-log data. However, it underestimates the paleo-flow depth (Bridge and Tye, 2000).

Climatic variations in time and space can induce a large variation in channel-belt thickness in rivers (Figs. 9, 10, and 11) of similar drainage basin area and statistical overlap of values for rivers with much different areas. The maximum channel-belt thickness of the paleo–Houston-Brazos and paleo-Guadalupe rivers is nearly equal to the minimum channel-belt thickness of the paleo–Mississippi River. This overlap may have resulted from measuring channel-belt thickness in different locations within a channel landform (e.g., thalweg versus depositional bank) or from periodic climate changes during the history of the

TABLE 3. PARAMETERS OF SOURCE-TO-SINK SYSTEMS OF THE LOWER MIOCENE INTERVAL IN THE NORTHERN GULF OF MEXICO

River system	Lower channel-belt thickness (m)	Bankfull thickness (m)	Shelf width (m)	Drainage basin length (km)	Drainage basin area (10^3 km^2)	Submarine fan run-out length (km)	Submarine fan area (km^2)
Mississippi	19.7	25	142	2650	1500	380	64,000
Red	16.1	21.1	92	1860	540	190	24,000
Rio Grande	11.2	17	115	1220	300	130	17,600
Houston-Brazos	9.1	13	75	450	100	N/A	N/A
Guadalupe	8.4	12.8	77	470	60	N/A	N/A

NA—No submarine fans were interpreted from current well log and seismic data.

river system. For small drainage systems, the peak water discharge can be several orders of magnitude higher than the long-term average rate (Mulder and Syvitski, 1995). Therefore, the flood stage of small systems can have a temporary channel-flow depth similar to that of much larger systems. In this work, we use average bankfull thickness to average these variations and use it to represent the long-term flow depth for the entire early Miocene period (~8 m.y.).

Additional uncertainty comes from burial compaction of channel-belt sediments. The compaction is complicated by many factors, including grain roundness, sorting, mineral composition, and size grading (Allen and Chilingarian, 1975). Ethridge and Schumm (1977) suggested a reduction of 10% of original bankfull depth by subsurface compaction. Our channel- belt data were compiled from various well-log data from the Texas-Louisiana coastal plain. Most channel-belt data were measured from units that are now lying between 100 m and 1000 m deep; a few channel-belt deposits are buried to a depth of 1500 m. It is not easy to give a simple decompaction correction for our channel-belt measurement because channel-belt deposits experienced different compaction histories. Overly simple correction for compaction may introduce extra uncertainties into system. Given that uncertainties in the statistical predictions lie in the range of one to two orders of magnitude, we conclude that compacted variability will not affect the predictions measurably; thus, we do not apply corrections.

In summary, natural S2S systems are complex (e.g., thickness variations in a single channel), and many uncertainties are associated with the measurements. Variations in tectonics and climate in catchment areas complicate the correlation between channel depth and drainage- basin area, resulting in uncertainties of more than an order of magnitude. However, these uncertainties are part of natural systems and are not flaws in methodology.

Given these uncertainties, it may be hard to differentiate a continental-scale drainage system from a large-scale drainage system by using channel-belt thickness alone. However, continental-scale systems rarely share the same channel dimensions with moderate-scale rivers or smaller systems (Figs. 9 and 10). Alternatively, detrital zircon U-Pb age spectra have been proven to be a useful approach for conducting provenance analyses and reconstructing paleogeography. However, detrital zircons can survive multiple recycling events, blurring or complicating the definition of specific source terranes, and they may sometimes fail to track intermediate source terranes. Combining detrital zircon provenance analysis and channel-belt measurement provides a better constraint on paleo–drainage basin area than does either technique alone.

CONCLUSIONS

Single-story channel-belt thicknesses were measured from an extensive well-log database in the well-explored GOM basin to calculate paleo-drainage areas of several differentiated early Miocene fluvial systems. Mean channel-belt thickness shows a strong correlation with paleo-drainage area that was reconstructed independently from petrographic and detrital zircon provenance analyses and continental geomorphic synthesis (Fig. 13B).

The drainage area was calculated from both mean lower channel-belt and mean bankfull thickness data, using scaling relationships that were built on a global modern and Quaternary river database. Drainage basin areas calculated from mean bankfull thickness show good agreement with independently mapped drainage basin areas (Table 2), although the measurement of bankfull thickness has high interpretive uncertainties when using well-log data alone. Using sandy lower channel-belt thickness, which is easy to identify from well-log response, resulted in smaller predicted areas that show much departure from the independently mapped drainage basin area and from the trend line of modern and Quaternary river data (Fig. 12; Table 2). Therefore, bankfull thickness is the better proxy for estimating paleo-channel depths and calculation of drainage basin area.

Drainage basin area predicted from mean bankfull thickness shows a wide range, more than an order of magnitude. The reconstructed drainage area of each well-studied early Miocene system lies between the minimum and maximum values, supporting the use of the modern data set to predict ancient unmappable drainage basin area. Combining detrital zircon provenance analyses and channel-belt measurements provides a better constraint on paleo–drainage basin area than does either technique alone.

Extrapolating the scaling relationship established on modern and Quaternary data into deep-time stratigraphy involves many uncertainties, including natural internal channel-belt thickness variation, incomplete channel preservation, subjective interpretation and measurement of channel-belt thickness, compaction overprints, and climatic and tectonic variability in catchment areas. However, these uncertainties do not negate the power of this scaling relationship. Knowledge of fluvial deposit dimensions, such as channel-belt thickness, provides a first-order estimate of drainage basin area and a plausible assessment of continental geomorphology.

Mean channel-belt bankfull depth correlates with drainage-basin length and area and submarine-fan length and area in early Miocene S2S systems. This correlation indicates a mass balance between sediment supply from catchment, sediment transport through fluvial channels, and sediment ultimately deposited in the basin. Therefore, knowledge of channel dimensions onshore also has implications for prediction of the dimensions of fan run-out length and area in the deep-water basin.

ACKNOWLEDGMENTS

We would like to thank the members of the GBDS industrial associate program and GBDS project manager Patricia Ganey-Curry. We thank the Institute for Geophysics, University of Texas at Austin, for providing a Ewing-Worzel Graduate Fellowship. Constructive comments by an anonymous reviewer and Peter Sadler are appreciated and helped greatly to improve this manuscript.

REFERENCES CITED

Allen, D.R., and Chilingarian, G.V., 1975, Mechanics of sand compaction, *in* Chilingarian, G.V., and Wolf, K.H., eds., Compaction of Coarse-Grained Sediments I: New York, Elsevier, Developments in Sedimentology, v. 18, p. 43–77, doi:10.1016/S0070-4571(08)71084-7.

Allen, P.A., 2008a, From landscapes into geological history: Nature, v. 451, p. 274–276, doi:10.1038/nature06586.

Allen, P.A., 2008b, Time scales of tectonic landscapes and their sediment routing systems, *in* Gallagher, K., Jones, S.J., and Wainwright, J., eds., Landscape Evolution: Denudation, Climate and Tectonics over Different Time and Space Scales: Geological Society of London Special Publication 296, p. 7–28, doi:10.1144/SP296.2.

Ambrose, W.A., Hentz, T.F., Bonnaffé, F., Loucks, R.G., Brown, L.F., Jr., Wang, F.P., and Potter, E.C., 2009, Sequence-stratigraphic controls on complex reservoir architecture of highstand fluvial-dominated deltaic and lowstand valley-fill deposits in the Upper Cretaceous (Cenomanian) Woodbine Group, East Texas field: Regional and local perspectives: American Association of Petroleum Geologists Bulletin, v. 93, p. 231–269, doi:10.1306/09180808053.

Anderson, J.B., Rodriguez, A., Abdulah, K.C., Fillon, R.H., Banfield, L.A., McKeown, H.A., and Wellner, J.S., 2004, Late Quaternary stratigraphic evolution of the northern Gulf of Mexico margin: A synthesis, *in* Anderson, J.B., and Fillon, R.H., eds., Late Quaternary Stratigraphic Evolution of the Northern Gulf of Mexico Margin: SEPM (Society for Sedimentary Geology) Special Publication 79, p. 1–23, doi:10.2110/pec.04.79.0001.

Anderson, J.B., Wallace, D.J., Simms, A.R., Rodriguez, A.B., and Milliken, K.T., 2014, Variable response of coastal environments of the northwestern Gulf of Mexico to sea-level rise and climate change: Implications for future change: Marine Geology, v. 352, p. 348–366, doi:10.1016/j.margeo.2013.12.008.

Anderson, J.B., Wallace, D.J., Simms, A.R., Rodriguez, A.B., Weight, R.W., and Taha, Z.P., 2016, Recycling sediments between source and sink during a eustatic cycle: Systems of late Quaternary northwestern Gulf of Mexico Basin: Earth-Science Reviews, v. 153, p. 111–138, doi:10.1016/j.earscirev.2015.10.014.

Baker, E.T., Jr., 1995, Stratigraphic nomenclature and geologic sections of the Gulf Coastal Plain of Texas: U.S. Geological Survey Open-File Report 94-461, 34 p.

Bebout, D.G., and Gutierrez, D.R., 1983, Regional cross sections, Louisiana Gulf Coast: Louisiana Geological Survey Folio Series 6, 10 p.

Bentley, S.J., Blum, M.D., Maloney, J., Pond, L., and Paulsell, R., 2016, The Mississippi River source-to-sink system: Perspectives on tectonic, climatic, and anthropogenic influences, Miocene to Anthropocene: Earth-Science Reviews, v. 153, p. 139–174, doi:10.1016/j.earscirev.2015.11.001.

Bernard, H.A., Major, C.F., Parrot, B.F., and LeBlanc, R.J., Sr., 1970, Recent sediments of southeast Texas: A field guide to the Brazos alluvial and deltaic plains and the Galveston Barrier Island Complex: The University of Texas at Austin, Bureau of Economic Geology Guidebook 11, 140 p.

Bhattacharya, J.P., and Tye, R.S., 2004, Searching for modern Ferron analogs and application to subsurface interpretation, *in* Chidsey, T.C. Jr., Adams, R.D., and Morris, T.H., eds., Regional to Wellbore Analog for Fluvial- Deltaic Reservoir Modeling: The Ferron Sandstone of Utah: American Association of Petroleum Geologists Studies in Geology 50, p. 39–57.

Bhattacharya, J.P., Copeland, P., Lawton, T.F., and Holbrook, J.H., 2016, Estimation of source area, river paleo-discharge, paleoslope, and sediment budgets of linked deep-time depositional systems and implications for hydrocarbon potential: Earth-Science Reviews, v. 153, p. 77–110, doi:10.1016/j.earscirev.2015.10.013.

Blum, M.D., and Roberts, H.H., 2012, The Mississippi delta region: Past, present, and future: Annual Review of Earth and Planetary Sciences, v. 40, p. 655–683, doi:10.1146/annurev-earth-042711-105248.

Blum, M.D., and Törnqvist, T.E., 2000, Fluvial responses to climate and sea-level change: A review and look forward: Sedimentology, v. 47, p. 2–48, doi:10.1046/j.1365-3091.2000.00008.x.

Blum, M.D., and Womack, J.H., 2009, Climate change, sea-level change, and fluvial sediment supply to deepwater systems, *in* Kneller, B., Martinsen, O.J., and McCaffrey, B., eds., External Controls on Deep Water Depositional Systems: Climate, Sea-Level, and Sediment Flux: SEPM (Society for Sedimentary Geology) Special Publication 92, p. 15–39, doi:10.2110/sepmsp.092.015.

Blum, M., Martin, B.J., Milliken, K., and Garvin, M., 2013, Paleovalley systems: Insights from quaternary analogs and experiments: Earth-Science Reviews, v. 116, p. 128–169, doi:10.1016/j.earscirev.2012.09.003.

Bridge, J.S., 2003, Rivers and Floodplains: Forms, Processes, and Sedimentary Record: Oxford, UK, Blackwell Science Ltd., 504 p.

Bridge, J.S., and Tye, R.S., 2000, Interpreting the dimensions of ancient fluvial channel bars, channels, and channel belts from wireline-logs and cores: American Association of Petroleum Geologists Bulletin, v. 84, p. 1205–1228, doi:10.1306/A9673C84-1738-11D7-8645000102C1865D.

Covault, J.A., Shelef, E., Traer, M., Hubbard, S.M., Romans, B.W., and Fildani, A., 2012, Deepwater channel run-out length: Insights from seafloor geomorphology: Journal of Sedimentary Research, v. 82, p. 21–36, doi:10.2110/jsr.2012.2.

Cox, R.T., Lumsden, D.N., and Van Arsdale, R.B., 2014, Possible relict meanders of the Pliocene Mississippi River and their implications: The Journal of Geology, v. 122, p. 609–622, doi:10.1086/676974.

Davidson, S.K., and Hartley, A.J., 2014, A quantitative approach to linking drainage area and distributive-fluvial-system area in modern and ancient endorheic basins: Journal of Sedimentary Research, v. 84, p. 1005–1020, doi:10.2110/jsr.2014.79.

Davidson, S.K., and North, C.P., 2009, Geomorphological regional curves for prediction of drainage area and screening modern analogues for rivers in the rock record: Journal of Sedimentary Research, v. 79, p. 773–792, doi:10.2110/jsr.2009.080.

Davies, D.K., Williams, B.P.J., and Vessell, R.K., 1993, Dimensions and quality of reservoirs originating in low and high sinuosity channel systems, Lower Cretaceous Travis Peak Formation, east Texas, USA, *in* North, C.P., and Prosser, D.J., eds., Characterization of Fluvial and Aeolian Reservoirs: Geological Society of London Special Publication 73, p. 95–121, doi:10.1144/GSL.SP.1993.073.01.07.

Dodge, M.M., and Posey, J.S., 1981, Structural cross sections, Tertiary formations, Texas Gulf Coast: Austin, The University of Texas at Austin, Bureau of Economic Geology, 6 p.

Durkin, P.R., Hubbard, S.M., Boyd, R.L., and Leckie, D.A., 2015, Stratigraphic expression of intrapoint-bar erosion and rotation: Journal of Sedimentary Research, v. 85, p. 1238–1257, doi:10.2110/jsr.2015.78.

Dutton, S.P., Loucks, R.G., and Day-Stirrat, R.J., 2012, Impact of regional variation in detrital mineral composition on reservoir quality in deep to ultradeep lower Miocene sandstones, western Gulf of Mexico: Marine and Petroleum Geology, v. 35, p. 139–153, doi:10.1016/j.marpetgeo.2012.01.006.

Ethridge, F.G., and Schumm, S.A., 1977, Reconstructing palaeochannel morphologic and flow characteristics: Methodology, limitations and assessment, *in* Miall, A.D., ed., Fluvial Sedimentology: Canadian Society of Petroleum Geology Memoir 5, p. 703–721.

Eversull, L.G., 1984, Regional cross sections, north Louisiana: Louisiana Geological Survey Folio 7, 10 p.

Feldman, H.R., Franseen, E.K., Joeckel, R.M., and Heckel, P.H., 2005, Impact of longer-term modest climate shifts on architecture of high-frequency sequences (cyclothems), Pennsylvanian of mid-continent U.S.A.: Journal of Sedimentary Research, v. 75, p. 350–368, doi:10.2110/jsr.2005.028.

Fielding, C.R., and Crane, R.C., 1987, An application of statistical modelling to the prediction of hydrocarbon recovery factors in fluvial reservoir sequences, *in* Ethridge, F.G., Flores, R.M., and Harvey, M.D., eds., Recent Developments in Fluvial Sedimentology: Society of Economic Paleontologists and Mineralogists Special Publication 39, p. 321–327, doi:10.2110/pec.87.39.0321.

Fisk, H.N., 1944, Geological investigation of the alluvial valley of the lower Mississippi River: Vicksburg, Mississippi, U.S. Army Corps of Engineers Mississippi River Commission, 78 p., 33 plates.

Foote, R.Q., Stoudt, D.L., Hutchinson, P.J., and Gordon, P.T., 1990, Gulf Coast regional cross section, east Texas–Texas coastal plain sector: Tulsa, Oklahoma, American Association of Petroleum Geologists, 3 sheets.

Frazier, D.E., and Osanik, A., 1961, Point-bar deposits, Old River Locksite, Louisiana: Gulf Coast Association of Geological Societies Transactions, v. 11, p. 121–137.

Galloway, W.E., 1981, Depositional architecture of Cenozoic Gulf Coastal Plain fluvial systems, *in* Etheridge, F.G., and Flores, R.M., eds., Recent and Ancient Nonmarine Depositional Environments: Society of Economic Paleontologists and Mineralogists Special Publication 31, p. 127–155, doi:10.2110/pec.81.31.0127.

Galloway, W.E., 1998, Siliciclastic slope and base-of-slope depositional systems: Component facies, stratigraphic architecture, and classification: American Association of Petroleum Geologists Bulletin, v. 82, p. 569–595.

Galloway, W.E., 2008, Depositional evolution of the Gulf of Mexico sedimentary basin, *in* Miall, A.D., ed., Sedimentary Basins of the World, Volume 5: The Sedimentary Basins of the United States and Canada: Amsterdam, Elsevier, p. 505–549, doi:10.1016/S1874-5997(08)00015-4.

Galloway, W.E., and Hobday, D.K., 1996, Terrigenous Clastic Depositional Systems: Applications to Fossil Fuel and Groundwater Resources: Heidelberg, Springer-Verlag, 489 p., doi:10.1007/978-3-642-61018-9.

Galloway, W.E., Henry, C.D., and Smith, G.E., 1982, Depositional framework, hydrostratigraphy, and uranium mineralization of the Oakville Sandstone (Miocene), Texas Coastal Plain: The University of Texas at Austin, Bureau of Economic Geology Report of Investigations 113, 51 p.

Galloway, W.E., Jirik, L.A., Morton, R.A., and Dubar, J.R., 1986, Lower Miocene (Fleming) depositional episode of the Texas Coastal Plain and continental shelf: Structural framework, facies, and hydrocarbon resources: The University of Texas at Austin, Bureau of Economic Geology Report of Investigations 150, 50 p.

Galloway, W.E., Ganey-Curry, P.E., Li, X., and Buffler, R.T., 2000, Cenozoic depositional history of the Gulf of Mexico basin: American Association of Petroleum Geologists Bulletin, v. 84, p. 1743–1774, doi:10.1306/8626C37F-173B-11D7-8645000102C1865D.

Galloway, W.E., Whiteaker, T.L., and Ganey-Curry, P., 2011, History of Cenozoic North American drainage basin evolution, sediment yield, and accumulation in the Gulf of Mexico basin: Geosphere, v. 7, p. 938–973, doi:10.1130/GES00647.1.

Ghinassi, M., and Ielpi, A., 2015, Stratal architecture and morphodynamics of downstream-migrating fluvial point bars (Jurassic Scalby Formation, UK): Journal of Sedimentary Research, v. 85, p. 1123–1137, doi:10.2110/jsr.2015.74.

Ghinassi, M., and Ielpi, A., 2016, Downstream-migrating fluvial point bars in the rock record: Sedimentary Geology, v. 334, p. 66–96, doi:10.1016/j.sedgeo.2016.01.005.

Gibling, M.R., 2006, Width and thickness of fluvial channel bodies and valley fills in the geological record: A literature compilation and classification: Journal of Sedimentary Research, v. 76, p. 731–770, doi:10.2110/jsr.2006.060.

Hoagstrom, C.W., Ung, V., and Taylor, K., 2014, Miocene rivers and taxon cycles clarify the comparative biogeography of North American highland fishes: Journal of Biogeography, v. 41, p. 644–658, doi:10.1111/jbi.12244.

Holbrook, J., and Wanas, H., 2014, A fulcrum approach to assessing source-to-sink mass balance using channel paleohydrologic parameters derivable from common fluvial data sets with an example from the Cretaceous of Egypt: Journal of Sedimentary Research, v. 84, p. 349–372, doi:10.2110/jsr.2014.29.

Hovius, N., 1998, Controls on sediment supply by large rivers, *in* Shanley, K.W., and McCabe, P.J., eds., Relative Role of Eustasy, Climate, and Tectonism in Continental Rocks: SEPM (Society for Sedimentary Geology) Special Publication 59, p. 2–16, doi:10.2110/pec.98.59.0002.

Hovius, N., and Leeder, M., 1998, Clastic sediment supply to basins: Basin Research, v. 10, p. 1–5, doi:10.1046/j.1365-2117.1998.00061.x.

Howard, A.D., 1958, Drainage evolution in northeastern Montana and northwestern North Dakota: Geological Society of America Bulletin, v. 69, p. 575–588, doi:10.1130/0016-7606(1958)69 [575:DEINMA]2.0.CO;2.

Hubbard, S.M., Smith, D.G., Nielsen, H., Leckie, D.A., Fustic, M., Spencer, R.J., and Bloom, L., 2011, Seismic geomorphology and sedimentology of a tidally influenced river deposit, Lower Cretaceous Athabasca oil sands, Alberta, Canada: American Association of Petroleum Geologists Bulletin, v. 95, p. 1123–1145, doi:10.1306/12131010111.

Labrecque, P.A., Jensen, J.L., and Hubbard, S.M., 2011, Cyclicity in Lower Cretaceous point bar deposits with implications for reservoir characterization, Athabasca Oil Sands, Alberta, Canada: Sedimentary Geology, v. 242, p. 18–33, doi:10.1016/j.sedgeo.2011.06.011.

Leeder, M.R., 1973, Fluviatile fining-upward cycles and the magnitude of paleochannels: Geological Magazine, v. 110, p. 265–276, doi:10.1017/S0016756800036098.

Leopold, L.B., and Maddock, T., 1953, The hydraulic geometry of stream channels and some physiographic implications: U.S. Geological Survey Professional Paper 252, 57 p.

Lorenz, J.C., Heinze, D.M., Clark, J.A., and Searls, C.A., 1985, Determination of widths of meander-belt sandstone reservoirs from vertical downhole data, Mesaverde Group, Piceance Creek basin, Colorado: American Association of Petroleum Geologists Bulletin, v. 69, p. 710–721.

Matthai, H.F., 1990, Floods, *in* Woolman, M.G., and Riggs, H.C., eds., Surface Water Hydrology: Boulder, Colorado, Geological Society of America, The Geology of North America, v. O-1, p. 97–120.

Metcalf, C., 2004, Regional channel characteristics for maintaining natural fluvial geomorphology in Florida streams: Panama City, Florida, U.S. Fish and Wildlife Service, Panama City Fisheries Resource Office, 41 p.

Miall, A.D., 2006, How do we identify big rivers? And how big is big?: Sedimentary Geology, v. 186, p. 39–50, doi:10.1016/j.sedgeo.2005.10.001.

Miall, A.D., 2010, Alluvial deposits, *in* James, N.P., and Dalrymple, R.W., eds., Facies Models 4: Geological Association of Canada Geotext 6, p. 105–137.

Miall, A.D., 2014, Large rivers and their depositional systems, *in* Miall, A.D., ed., Fluvial Depositional Systems: Springer, p. 273–294, doi:10.1007/978-3-319-00666-6_7.

Milliman, J.D., and Syvitski, J.P.M., 1992, Geomorphic tectonic control of sediment discharge to the ocean: The importance of small mountainous rivers: The Journal of Geology, v. 100, p. 525–544, doi:10.1086/629606.

Moody, T., Wirtanen, M., and Yard, S.N., 2003, Regional relationships for bankfull stage in natural channels of the arid southwest: Flagstaff, Arizona, Natural Channel Design Inc., 36 p.

Mulder, T., and Syvitski, J.P.M., 1995, Turbidity currents generated at river mouths during exceptional discharges to the world oceans: The Journal of Geology, v. 103, p. 285–299, doi:10.1086/629747.

Nicholas, A.P., Smith, G.H.S., Amsler, M.L., Ashworth, P.J., Best, J.L., Hardy, R.J., Lane, S.N., Orfeo, O., Parsons, D.R., Reesink, A.J.H., Sandbach, S.D., Simpson, C.J., and Szupiany, R.N., 2016, The role of discharge variability in determining alluvial stratigraphy: Geology, v. 44, p. 3–6, doi:10.1130/G37215.1.

Olariu, C., and Bhattacharya, J.P., 2006, Terminal distributary channels and delta front architecture of river-dominated delta systems: Journal of Sedimentary Research, v. 76, p. 212–233, doi:10.2110/jsr.2006.026.

Romans, B.W., and Graham, S.A., 2013, A deep-time perspective of land-ocean linkages in the sedimentary record: Annual Review of Marine Science, v. 5, p. 69–94, doi:10.1146/annurev-marine-121211-172426.

Romans, B.W., Castelltort, S., Covault, J.A., Fildani, A., and Walsh, J.P., 2016, Environmental signal propagation in sedimentary systems across timescales: Earth-Science Reviews, v. 153, p. 7–29, doi:10.1016/j.earscirev.2015.07.012.

Sadler, P.M., and Jerolmack, D.J., 2015, Scaling laws for aggradation, denudation and progradation rates: The case for time-scale invariance at sediment sources and sinks, *in* Smith, D.G., Bailey, R.J., Burgess, P.M., and Fraser, A.J., eds., Strata and Time: Probing the Gaps in Our Understanding: Geological Society of London Special Publication 404, p. 69–88, doi:10.1144/SP404.7.

Saucier, R.T., 1994, Geomorphology and quaternary geologic history of the Lower Mississippi Valley: Vicksburg, Mississippi, U.S. Army Corps of Engineers, Waterways Experiment Station, 205 p.

Sears, J.W., 2013, Late Oligocene–early Miocene Grand Canyon: A Canadian connection?: GSA Today, v. 23, no. 11, p. 4–10, doi:10.1130/GSATG178A.1.

Smith, D.G., Hubbard, S., Leckie, D., and Fustic, M., 2009, Counter point bar deposits: Lithofacies and reservoir significance in the meandering modern Peace River and ancient McMurray Formation, Alberta, Canada: Sedimentology, v. 56, p. 1655–1669, doi:10.1111/j.1365-3091.2009.01050.x.

Smith, D.G., Hubbard, S.M., Lavigne, J.R., Leckie, D.A., and Fustic, M., 2011, Stratigraphy of counter-point-bar and eddy-accretion deposits in low energy meander belts of the Peace-Athabasca delta, northeast Alberta, Canada, *in* Davidson, S.K., Leleu, S., and North, C.P., eds., From River to Rock Record: The Preservation of Fluvial Sediments and Their Subsequent Interpretation: SEPM (Society for Sedimentary Geology) Special Publication 97, p. 143–152, doi:10.2110/sepmsp.097.143.

Snedden, J.W., 1984, Validity of the use of the spontaneous potential curve shape in the interpretation of sandstone depositional environments: Gulf Coast Association of Geological Societies Transactions, v. 34, p. 255–263.

Snedden, J.W., Galloway, W.E., Whiteaker, T.L., and Ganey-Curry, P.E., 2012, Eastward shift of deepwater fan axes during the Miocene in the Gulf of Mexico: Possible causes and models: Gulf Coast Association of Geological Societies Journal, v. 1, p. 131–144.

Sømme, T.O., Helland-Hansen, W., Martinsen, O.J., and Thurmond, J.B., 2009a, Relationships between morphological and sedimentological parameters in source-to-sink systems: A basis for predicting semi-quantitative characteristics in subsurface systems: Basin Research, v. 21, p. 361–387, doi:10.1111/j.1365-2117.2009.00397.x.

Sømme, T.O., Martinsen, O.J., and Thurmond, J.B., 2009b, Reconstructing morphological and depositional characteristics in subsurface sedimentary systems: An example from the Maastrichtian-Danian Ormen Lange system, Møre Basin, Norwegian Sea: American Association of Petroleum Geologists Bulletin, v. 93, p. 1347–1377, doi:10.1306/06010909038.

Spradlin, S.D., 1980, Miocene fluvial systems: Southeast Texas [M.S. thesis]: Austin, University of Texas at Austin, 139 p.

Strauss, D., and Sadler, P.M., 1989, Stochastic models for the completeness of stratigraphic sections: Journal of the International Association for Mathematical Geology, v. 21, p. 37–59, doi: 10.1007/BF00897239.

Syvitski, J.P.M., and Milliman, J.D., 2007, Geology, geography, and humans battle for dominance over the delivery of fluvial sediment to the coastal ocean: The Journal of Geology, v. 115, p. 1–19, doi:10.1086/509246.

Tye, R.S., 1991, Fluvial-sandstone reservoirs of the Travis Peak Formation, East Texas basin, *in* Miall, A.D., and Tyler, N., eds., The Three-Dimensional Facies Architecture of Terrigenous Clastic Sediments and Its Implications for Hydrocarbon Discovery and Recovery: SEPM (Society for Sedimentary Geology) Concepts in Sedimentology and Paleontology 3, p. 172–188, doi:10.2110/csp.91.03.0172.

Wetzel, A., 1993, The transfer of river load to deep-sea fans: A quantitative approach: American Association of Petroleum Geologists Bulletin, v. 77, p. 1679–1692.

Willis, B.J., 1989, Paleochannel reconstructions from point bar deposits: A three-dimensional perspective: Sedimentology, v. 36, p. 757–766, doi:10.1111/j.1365-3091.1989.tb01744.x.

Willis, B.J., and Tang, H., 2010, Three-dimensional connectivity of point-bar deposits: Journal of Sedimentary Research, v. 80, p. 440–454, doi:10.2110/jsr.2010.046.

Wolman, M.G., and Leopold, L.B., 1957, River floodplains: Some observations on their formation: U.S. Geological Survey Professional Paper 282-C, p. 87–107.

Wolman, M.G., and Miller, J.P., 1960, Magnitude and frequency of forces in geomorphic processes: The Journal of Geology, v. 68, p. 54–74, doi:10.1086/626637.

Xu, J., Snedden, J.W., Stockli, D.F., Fulthorpe, C.S., and Galloway, W.E., 2016, Early Miocene continental-scale sediment supply to the Gulf of Mexico Basin based on detrital zircon analysis: Geological Society of America Bulletin, doi:10.1130/B31465.1.

Young, S.C., Budge, T., Knox, P.R., Kalbouss, R., Baker, E.T., Jr., Hamlin, H.S., Galloway, W.E., and Deeds, N., 2010, Hydrostratigraphy of the Gulf Coast Aquifer from the Brazos River to the Rio Grande: Austin, Texas Water Development Board, 231 p.

Young, S.C., Ewing, T., Hamlin, S., Baker, E., and Lupton, D., 2012, Final report updating the hydrogeologic framework for the northern portion of the Gulf Coast aquifer: Austin, Texas Water Development Board, 285 p.